J Math Chem (2014) 52:1717–1750
DOI 10.1007/s10910-014-0344-y

ORIGINAL PAPER

Symmetry-itemized enumeration of *RS*-stereoisomers of allenes. I. The fixed-point matrix method of the USCI approach combined with the stereoisogram approach

Shinsaku Fujita

Received: 6 February 2014 / Accepted: 25 February 2014 / Published online: 11 March 2014

Abstract After the *RS*-stereoisomeric group $\mathbf{D}_{2d\tilde{\sigma}\hat{I}}$ of order 16 has been defined by starting point group $\mathbf{D}_{2d}$ of order 8, the isomorphism between $\mathbf{D}_{2d\tilde{\sigma}\hat{I}}$ and the point group $\mathbf{D}_{4h}$ of order 16 is thoroughly discussed. The non-redundant set of subgroups (SSG) of $\mathbf{D}_{2d\tilde{\sigma}\hat{I}}$ is obtained by referring to the non-redundant set of subgroups of $\mathbf{D}_{4h}$. The coset representation for characterizing the orbit of the four positions of an allene skeleton is clarified to be $\mathbf{D}_{2d\tilde{\sigma}\hat{I}}(/\mathbf{C}_{s\tilde{\sigma}\hat{I}})$, which is closely related to the $\mathbf{D}_{4h}(/\mathbf{C}'''_{2v})$. According to the unit-subduced-cycle-index (USCI) approach (Fujita, Symmetry and combinatorial enumeration of chemistry. Springer, Berlin 1991), the subduction of $\mathbf{D}_{2d\tilde{\sigma}\hat{I}}(/\mathbf{C}_{s\tilde{\sigma}\hat{I}})$ is examined so as to generate unit subduced cycle indices with chirality fittingness (USCI-CFs). Then, the fixed-point matrix method of the USCI approach is applied to the USCI-CFs. Thereby, the numbers of quadruplets are calculated in an itemized fashion with respect to the subgroups of $\mathbf{D}_{2d\tilde{\sigma}\hat{I}}$. After the subgroups of $\mathbf{D}_{2d\tilde{\sigma}\hat{I}}$ are categorized into types I–V, type-itemized enumeration of quadruplets is conducted to illustrate the versatility of the stereoisogram approach.

Keywords Fixed-point matrix method · Allene · Enumeration · Chirality fittingness · Stereoisogram · *RS*-stereoisomeric group

1 Introduction

1.1 Point groups in stereochemistry

In most textbooks on organic stereochemistry, point groups are introduced to characterize total features of molecules. For example, the point group $\mathbf{D}_{2d}$ is introduced

S. Fujita (✉)
Shonan Institute of Chemoinformatics and Mathematical Chemistry, Kaneko 479-7 Ooimachi, Ashigara-Kami-Gun, Kanagawa-Ken 258-0019, Japan
e-mail: shinsaku_fujita@nifty.com

to characterize allene, spiro[4,4]nonane, and so on (e.g., Fig. 3.14 of [1], Fig. 3.6.4 of [2], and Fig. 4.39 of [3]). Inner features of molecules are treated in the form of orbitals (orbital functions) in quantum chemistry where linear (matrix) representations are mainly used [4]. In particular, symmetry adapted linear combinations (SALCs) of basis functions are constructed by utilizing projection operators after reducing a matrix representation into irreducible representations [4,5]. After linear representations are linked with coset representations, SALCs have been alternatively constructed by applying the coset representations [6], where the $\mathbf{D}_{2d}$-symmetry of allene is discussed as an example. More detailed discussions on the relationship between linear representations and coset representations have appeared in a recent monograph [7].

The set-of-coset-representation (SCR) notation based on coset representations has been proposed to differentiate molecules belonging to the same point group [8]. For example, the SCR notation $\mathbf{D}_{2d}[/\mathbf{C}_s(\mathrm{H}_4);\ /\mathbf{C}_{2v}(\mathrm{C}_2);\ /\mathbf{D}_{2d}(\mathrm{C})]$ is assigned to allene, because there appear a four-membered orbit (not orbital!) governed by the coset representation $\mathbf{D}_{2d}(/\mathbf{C}_s)$, a two-membered orbit governed by the coset representation $\mathbf{D}_{2d}(/\mathbf{C}_{2v})$, and a one-membered orbit governed by the coset representation $\mathbf{D}_{2d}(/\mathbf{D}_{2d})$ in an allene molecule (Table 11 of [8]). The SCI notation covers inner (local) symmetries ($\mathbf{C}_s$, $\mathbf{C}_{2v}$, and $\mathbf{D}_d$) along with the total features ($\mathbf{D}_{2d}$) of the allene molecule.

1.2 The USCI approach based on concepts concerning coset representations

Each orbit is characterized to be homospheric, enantiospheric, and hemispheric according to the corresponding coset representation [9]. The terms *homospheric*, *enantiospheric*, and *hemispheric* have attributive nature for characterizing the properties (attributes) of an orbit. According to its sphericity, the orbit exhibits chirality fittingness, which determines the packing of proligands in the orbit. In contrast, such conventional terms as ‘equivalent’, ‘enantiotopic’, and ‘diastereotopic’ [10] have relational nature, so that the concept of chirality fittingness cannot be deduced in a rational process.

According to its sphericity, each orbit is characterized by a sphericity index (a_d, c_d or b_d). The derivation of a molecule from a given skeleton (e.g. an allene skeleton) is described in terms of the concept of subduction of coset representations, where each orbit contained originally in the skeleton is divided into one or more orbits. For the purpose of discussing the behaviors of such orbits, the product of sphericity indices is calculated to give a unit subduced cycle index with chirality fittingness (USCI-CF). On the basis of USCI-CFs, four methods of enumeration have been developed and they are called *the unit-subduced-cycle-index (USCI) approach* collectively [11].

Among the four methods of the USCI approach [11], the fixed-point matrix (FPM) method has been applied to the enumeration of allene derivatives after the formulation of the proligand-promolecule model [12]. Promolecules derived from an allene skeleton have been enumerated and listed in a tabular form (Fig. 2.5 of [11] and Fig. 5 of [12]), where itemization to point-group symmetries has been conducted with respect to the point group $\mathbf{D}_{2d}$. In order to enumerate nonrigid three-dimensional-structural isomers, substituted methyl ligands have been substituted for proligands for allene derivatives, where ligand symmetries have been taken into consideration [13].

The partial-cycle-index (PCI) method is another versatile method of the USCI approach, which is based on generating function [11]. Generalization of partial cycle indices has been reported to enumerate achiral and chiral derivatives where a general procedure is exemplified by using an allene skeleton [14]

The concept of doubly-colored graphs has been discussed as graphical models for subductions of coset representations, double cosets, and unit subduced cycle indices, where allene derivatives are used as representative examples [15].

1.3 The concept of Mandalas and Fujita's proligand method

Importance of regular representations and regular bodies for characterizing orbits in a molecule has been demonstrated by using allene derivatives as examples [16]. The concept of mandalas as nested regular bodies has been proposed to characterize orbits among molecule by using allene derivatives as examples [17]. The USCI approach has been thoroughly discussed on the basis of the concept of mandalas, where orbits in molecules are linked with orbits among molecules by using allene derivatives as examples [18]. There has appeared a monograph concerning the concept of mandalas [19].

The concept of sphericity indices of cycles has been formulated to develop Fujita's proligand method as a stereochemical extension of Pólya's theorem, where allene derivatives are used as representative examples [20]. Fujita's proligand method has been detailedly discussed in a monograph [7].

Mandalas and Fujita's proligand method have been discussed [21]. The concept of mandalas has been discussed by using allene derivatives as examples from a group-theoretical point of view, so that it serves as diagrammatical expressions for characterizing symmetries of stereoisomers [22].

1.4 Stereoisograms and *RS*-stereoisomeric groups

Allene derivatives have been enumerated under the point group $\mathbf{D}_{2d}$ and compared with an alternative enumeration under a permutation group of degree 4, which is isomorphic to the point group $\mathbf{D}_{2d}$. The difference between the resulting isomer numbers has been discussed in terms of isomer equivalence [23]. Stereogenicity/astereogenicity, which is now recognized as *RS*-stereogenicity/*RS*-astereogenicity, has been formulated from the viewpoint of global/local permutation-group symmetry. The concept of *RS*-stereogenicity/*RS*-astereogenicity is discussed by using allene derivatives as examples [24].

On the basis of the proligand-promolecule model [12], the concept of *stereoisograms* has been proposed by Fujita to discuss stereogenicity and chirality comprehensively [25]. Thereby, it has been clarified that the conventional stereogenicity should be replaced by a more definite term, i.e., *RS-stereogenicity*, for the purpose of comparing it with chirality [26]. Each stereoisogram consists of a quadruplet of *RS*-stereoisomers, i.e., a reference promolecule, an enantiomer, an *RS*-diastereomer, and a holantimer. In particular, the proposal of holantimers enables us to discuss pseudoasymmetry, *RS*-stereogenicity, chirality, and the Cahn–Ingold–Prelog (CIP) system of RS-nomenclature [27–30] as well as on prochirality [31–35] in an integrated fashion.

It should be noted that anyone of the four promolecules contained in a quadruplet can be regarded as an alternative reference promolecule, which provides an equivalent stereoisogram to the original one. This means that the properties of a reference promolecule selected rather arbitrarily can be regarded as the properties of the stereoisogram at issue.

Point Groups, *RS*-stereoisomeric groups, stereoisomeric groups, and isoskeletal groups for characterizing allene derivatives have been discussed on the basis of the stereoisogram approach [36]. The existence of five types of stereoisograms has been proven on the basis of the existence of five types of subgroups of *RS*-stereoisomeric groups, where allene derivatives are used as representative examples [37]. Chirality and *RS*-stereogenicity of allene derivatives have been discussed on the basis of stereoisograms, where allene derivatives of five types are listed in tabular forms (Figs. 8–10 of [38]).

1.5 Aims of the present paper

In order to integrate the USCI approach and the stereoisogram approach, the present paper is devoted to enumeration of allene derivatives, which are regarded as quadruplets of promolecules contained in stereoisograms under the action of *RS*-stereoisomeric groups derived from the point group $\mathbf{D}_{2d}$. Because the $\mathbf{D}_{4h}$-point group is isomorphic to the *RS*-stereoisomeric group of an allene skeleton, the data of $\mathbf{D}_{4h}$ are applied to characterize the *RS*-stereoisomeric group derived from the point group $\mathbf{D}_{2d}$.

2 *RS*-stereoisomeric groups for allene derivatives

An allene skeleton is discussed by using a top projection **1** in place of a usual projection **2**, as shown in Fig. 1. The skeleton **1** (or **2**) is controlled by a point group $\mathbf{D}_{2d}$ (order 8), which can be extended into the corresponding *RS*-stereoisomeric group $\mathbf{D}_{2d\widetilde{\sigma}\widehat{I}}$ (order 16), as listed in Table 1.

The *RS*-stereoisomeric group $\mathbf{D}_{2d\widetilde{\sigma}\widehat{I}}$ has a normal subgroup $\mathbf{D}_2$ (order 4), which is also a normal subgroup of $\mathbf{D}_{2d}$. Hence, the $\mathbf{D}_{2d\widetilde{\sigma}\widehat{I}}$-group is decomposed into cosets as follows:

$$\mathbf{D}_{2d\widetilde{\sigma}\widehat{I}} = \mathbf{D}_2 + \sigma\mathbf{D}_2 + \widetilde{\sigma}\mathbf{D}_2 + \widehat{I}\mathbf{D}_2, \tag{1}$$

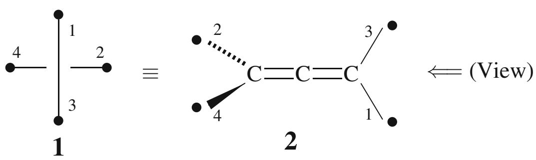

Fig. 1 Convention for drawing allene derivatives

Table 1 Operations of $\mathbf{D}_{2d\widetilde{\sigma}\widehat{I}}$ and coset representation of $\mathbf{D}_{2d\widetilde{\sigma}\widehat{I}}(/\mathbf{C}_{s\widetilde{\sigma}\widehat{I}})$ versus operations of $\mathbf{D}_{4h}$ and coset representation of $\mathbf{D}_{4h}(/\mathbf{C}'''_{2v})$

operation $g \in \mathbf{D}_{4h}$	operation $g \in \mathbf{D}_{2d\widetilde{\sigma}\widehat{I}}$	$\mathbf{D}_{4h}(/\mathbf{C}'''_{2v})$ or $\mathbf{D}_{2d\widetilde{\sigma}\widehat{I}}(/\mathbf{C}_{s\widetilde{\sigma}\widehat{I}})$ (product of cycles)	operation $g \in \mathbf{D}_{4h}$	operation $g \in \mathbf{D}_{2d\widetilde{\sigma}\widehat{I}}$	$\mathbf{D}_{4h}(/\mathbf{C}'''_{2v})$ or $\mathbf{D}_{2d\widetilde{\sigma}\widehat{I}}(/\mathbf{C}_{s\widetilde{\sigma}\widehat{I}})$ (product of cycles)
I	I	$(1)(2)(3)(4)$	$C'_{2(1)}$	$\widetilde{\sigma}_{d(1)}$	$(1)(2\ 4)(3)$
$C_{2(3)}$	$C_{2(3)}$	$(1\ 3)(2\ 4)$	$C'_{2(2)}$	$\widetilde{\sigma}_{d(2)}$	$(1\ 3)(2)(4)$
$C_{2(1)}$	$C_{2(1)}$	$(1\ 2)(3\ 4)$	C_4	$\widetilde{S}_4$	$(1\ 2\ 3\ 4)$
$C_{2(2)}$	$C_{2(2)}$	$(1\ 4)(2\ 3)$	C_4^3	$\widetilde{S}_4^3$	$(1\ 4\ 3\ 2)$
$\sigma_{d(1)}$	$\sigma_{d(1)}$	$\overline{(1)(2\ 4)(3)}$	σ_h	$\widehat{I}$	$\overline{(1)(2)(3)(4)}$
$\sigma_{d(2)}$	$\sigma_{d(2)}$	$\overline{(1\ 3)(2)(4)}$	i	$\widehat{C}_{2(3)}$	$\overline{(1\ 3)(2\ 4)}$
S_4	S_4	$\overline{(1\ 2\ 3\ 4)}$	$\sigma_{v(1)}$	$\widehat{C}_{2(1)}$	$\overline{(1\ 2)(3\ 4)}$
S_4^3	S_4^3	$\overline{(1\ 4\ 3\ 2)}$	$\sigma_{v(2)}$	$\widehat{C}_{2(2)}$	$\overline{(1\ 4)(2\ 3)}$

which has been noted previously (Eq. 4 of [37]). Note that the point group $\mathbf{D}_{2d}$ for the reference allene skeleton is decomposed as follows:

$$\mathbf{D}_{2d} = \mathbf{D}_2 + \sigma\mathbf{D}_2, \tag{2}$$

where the symbol σ is a representative selected from the four (roto)reflection operations of $\mathbf{D}_{2d}$. The coset decomposition shown by Eq. 2 characterizes an enantiomeric relationship.

In addition, there appears a subgroup of order 8 for characterizing an *RS*-diastereomeric relationship:

$$\mathbf{D}_{2\widetilde{\sigma}} = \mathbf{D}_2 + \widetilde{\sigma}\mathbf{D}_2, \tag{3}$$

which has been noted previously (Eq. 3 of [37]). Note that the symbol $\widetilde{\sigma}$ represents an operation which has the same permutation as σ but no alternation of chirality. Another subgroup of order 8 characterizes a holantimeric relationship:

$$\mathbf{D}_{2\widehat{I}} = \mathbf{D}_2 + \widehat{I}\mathbf{D}_2, \tag{4}$$

which has been noted previously (Eq. 2 of [37]). Note that the symbol $\widehat{I}$ represents an operation which has the same permutation as I but alternation of chirality.

The operations of $\mathbf{D}_{2d\widetilde{\sigma}\widehat{I}}$ are summarized in the $\mathbf{D}_{2d\widetilde{\sigma}\widehat{I}}$-columns of Table 1. The upper-left part marked by the gray letter **A** collects the operations of the normal subgroup $\mathbf{D}_{2d}$, the lower-left part marked by the gray letter **B** collects the operations of the coset $\sigma\mathbf{D}_2$ $(= \mathbf{D}_{2d} - \mathbf{D}_2)$ (cf. Eq. 2), the upper-right part marked by the gray letter **C** collects the operations of the coset $\widetilde{\sigma}\mathbf{D}_2$ $(= \mathbf{D}_{2\widetilde{\sigma}} - \mathbf{D}_2)$ (cf. Eq. 3), and the lower-right part marked by the gray letter **D** collects the operations of the coset $\widehat{I}\mathbf{D}_2$ $(= \mathbf{D}_{2\widehat{I}} - \mathbf{D}_2)$ (cf. Eq. 4). Hence, Eqs. 1–4 are alternatively represented in the form of sets of operations:

$$\mathbf{D}_{2d\widetilde{\sigma}\widehat{I}} = \{\mathbf{A}, \mathbf{B}, \mathbf{C}, \mathbf{D}\} \tag{5}$$
$$\mathbf{D}_{2d} = \{\mathbf{A}, \mathbf{B}\} \tag{6}$$
$$\mathbf{D}_{2\widetilde{\sigma}} = \{\mathbf{A}, \mathbf{C}\} \tag{7}$$
$$\mathbf{D}_{2\widehat{I}} = \{\mathbf{A}, \mathbf{D}\} \tag{8}$$
$$\mathbf{D}_{2} = \{\mathbf{A}\}, \tag{9}$$

where the cosets **A**, **B**, **C**, and **D** contain the operations listed in the $\mathbf{D}_{2d\widetilde{\sigma}\widehat{I}}$-columns of Table 1. It should be noted that each operation of **A** corresponds to an operation of **D**, where the correspondence is shown by the absence or presence of a hat accent. In a similar way, each operation of **B** corresponds to an operation of **C**, where the correspondence is shown by the absence or presence of a tilde accent.

Each of the four cosets shown in the right-hand side of Eq. 1 corresponds to one component of a quadruplet of *RS*-stereoisomers, i.e., $\mathbf{D}_2$ to a reference skeleton, $\sigma\mathbf{D}_2$ $(= \mathbf{D}_{2d} - \mathbf{D}_2)$ to its enantiomeric skeleton, $\widetilde{\sigma}\mathbf{D}_2$ $(= \mathbf{D}_{2\widetilde{\sigma}} - \mathbf{D}_2)$ to its *RS*-diastereomeric skeleton, and $\widehat{I}\mathbf{D}_2$ $(= \mathbf{D}_{2\widehat{I}} - \mathbf{D}_2)$ to its holantimeric skeleton. Thereby, a quadruplet of *RS*-stereoisomers is selected as shown in Fig. 2a, where an appropriate representative is selected according to each coset of Eq. 1, i.e.,

$$\begin{array}{llll}
\mathbf{1} & \text{for} & I\,(\in \mathbf{D}_2) & \sim (1)(2)(3)(4), \\
\overline{\mathbf{1}} & \text{for} & \sigma_{d(1)}\ (\in \sigma\mathbf{D}_2 = \mathbf{D}_{2d} - \mathbf{D}_2) & \sim \overline{(1)(2\,4)(3)}, \\
\mathbf{3} & \text{for} & \widetilde{\sigma}_{d(1)}\ (\in \widetilde{\sigma}\mathbf{D}_2 = \mathbf{D}_{2\widetilde{\sigma}} - \mathbf{D}_2) & \sim (1)(2\,4)(3), \text{ and} \\
\overline{\mathbf{3}} & \text{for} & \widehat{I}\ \ (\in \widehat{I}\mathbf{D}_2 = \mathbf{D}_{2\widehat{I}} - \mathbf{D}_2) & \overline{(1)(2)(3)(4)}.
\end{array}$$

The resulting diagram (Fig. 2a) is here called a *reference stereoisogram*. Strictly speaking, each skeleton collected in Fig. 2a corresponds to a representative of the

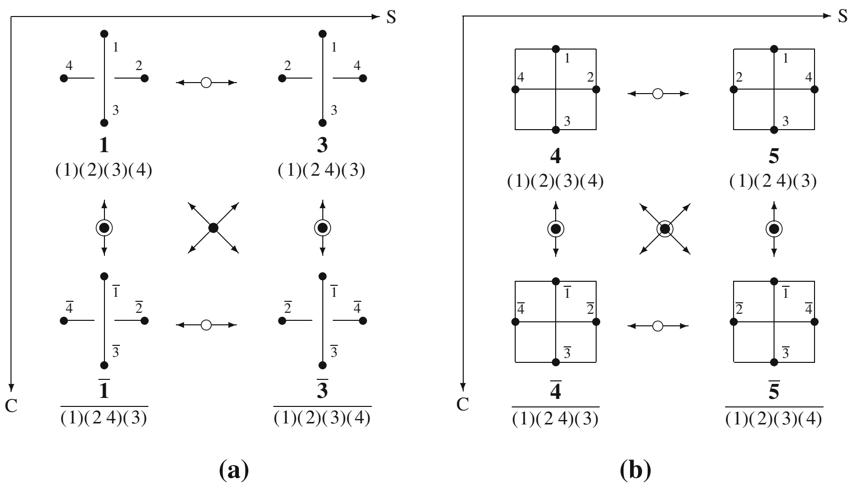

Fig. 2 Reference stereoisogram for an allene skeleton (**a**) and point-group symmetry of a square-planar skeleton (**b**)

corresponding coset, i.e., I ($\in \mathbf{D}_2$) for **1**, $\sigma_{d(1)}$ ($\in \sigma\mathbf{D}_2 = \mathbf{D}_{2d} - \mathbf{D}_2$) for $\overline{\mathbf{1}}$, $\widetilde{\sigma}_{d(1)}$ ($\in \widetilde{\sigma}\mathbf{D}_2 = \mathbf{D}_{2\widetilde{\sigma}} - \mathbf{D}_2$) for **3**, $\widehat{I}$ ($\in \widehat{I}\mathbf{D}_2 = \mathbf{D}_{2\widehat{I}} - \mathbf{D}_2$) for $\overline{\mathbf{3}}$. It should be noted that each representative skeleton (**1**, $\overline{\mathbf{1}}$, **3**, or $\overline{\mathbf{3}}$) is converted into its homomer under the action of $\mathbf{D}_2$, where the mode of numbering is altered according to $\mathbf{D}_2$ so as to result in the numbering due to the respective coset.

The operations of the $\mathbf{D}_{2d}$ collected in the **A**- and **B**-part of Table 1 correspond to respective products of cycles, which are contained in the coset representation $\mathbf{D}_{2d}(/\mathbf{C}_s)$ [37]. The products of cycles corresponding to the operations collected in the **C**- and **D**-parts have been originally assigned by taking account of the correspondence between $\sigma\mathbf{D}_2$ and $\widetilde{\sigma}\mathbf{D}_2$ or between $\mathbf{D}_2$ and $\widehat{I}\mathbf{D}_2$, where an overline is attached or not (e.g., $(1)(2)(3)(4)$ vs. $\overline{(1)(2)(3)(4)}$ and $\overline{(1)(2\,4)(3)}$ vs. $(1)(2\,4)(3)$) to each product of cycles and a tilde (or hat) accent is attached or not to each operation (e.g., I vs. $\widehat{I}$ and $\sigma_{d(1)}$ vs. $\widetilde{\sigma}_{d(1)}$). This means that the products of cycles reported originally in [37] have not directly derived from the coset representation concerning the *RS*-stereoisomeric group $\mathbf{D}_{2d\widetilde{\sigma}\widehat{I}}$. Hence, the products of cycles should be redefined as the elements of the coset representation $\mathbf{D}_{2d\widetilde{\sigma}\widehat{I}}(/\mathbf{C}_{s\widetilde{\sigma}\widehat{I}})$ after the isomorphism between the point group $\mathbf{D}_{4h}$ and the *RS*-stereoisomeric group $\mathbf{D}_{2d\widetilde{\sigma}\widehat{I}}$ is taken into consideration.

3 Point groups isomorphic to *RS*-stereoisomeric groups

3.1 Symmetry elements of $\mathbf{D}_{2d\widetilde{\sigma}\widehat{I}}$ and those of $\mathbf{D}_{4h}$

According to the definition of $\mathbf{D}_{2d\widetilde{\sigma}\widehat{I}}$, the $\mathbf{D}_{2d}$-part (**A** and **B**) of $\mathbf{D}_{2d\widetilde{\sigma}\widehat{I}}$ is isomorphic to (the same as) the $\mathbf{D}_{2d}$-part of $\mathbf{D}_{4h}$. The remaining parts (**C** and **D**) exhibit the correspondence shown in Table 1, so that the *RS*-stereoisomeric group $\mathbf{D}_{2d\widetilde{\sigma}\widehat{I}}$ is totally isomorphic to the point group $\mathbf{D}_{4h}$. The symmetry elements of the point group $\mathbf{D}_{2d}$ along with those of the *RS*-stereoisomeric group $\mathbf{D}_{2d\widetilde{\sigma}\widehat{I}}$ are depicted in the left diagram of Fig. 3 (**6**), where the symbols for the symmetry elements of $\mathbf{D}_{2d\widetilde{\sigma}\widehat{I}}$ (not of $\mathbf{D}_{2d}$) are shown in pairs of brackets.

As summarized in Table 1, the symmetry elements without a tilde or hat accent in the left diagram of Fig. 3 (**6**) depict rotation or rotoreflection axes, which construct the point group $\mathbf{D}_{2d}$ ($\subset \mathbf{D}_{2d\widetilde{\sigma}\widehat{I}}$). For example, the S_4-axis shown as a perpendicular

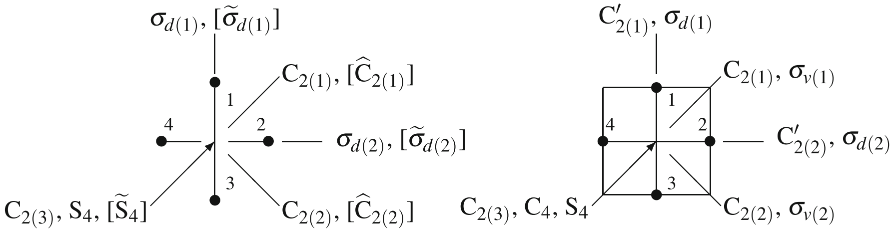

Fig. 3 Symmetry elements of the point group $\mathbf{D}_{2d}$ (and $\mathbf{D}_{2d\widetilde{\sigma}\widehat{I}}$) for characterizing an allene skeleton (**6**) as well as symmetry elements of the point group $\mathbf{D}_{4h}$ for characterizing a square-planar skeleton (**7**)

axis in **6** is a common symmetry element to $\mathbf{D}_{2d}$, so that it generates the operations S_4, $C_{2(3)}$ $(= S_4^2)$, and S_4^3, where it implies the presence of the $C_{2(3)}$-axis.

The symmetry elements with a tilde or hat accent construct the coset $\mathbf{D}_{2d\widetilde{\sigma}\widehat{I}} - \mathbf{D}_{2d}$ (i.e., $\{\mathbf{C}, \mathbf{D}\}$). The symbol $[\widetilde{\mathrm{S}}_4]$ with a pair of brackets in **6** indicates the presence of the $\widetilde{\mathrm{S}}_4$-axis as a symmetry element of $\mathbf{D}_{2d\widetilde{\sigma}\widehat{I}}$, which generates the operations $\widetilde{S}_4$, $C_{2(3)}$ $(= \widetilde{S}_4^2)$, and $\widetilde{S}_4^3$.

On the other hand, the symmetry elements of the point group $\mathbf{D}_{4h}$ are depicted in the right diagram of Fig. 3 (**7**), where the inversion center (i) and the horizontal mirror plane (σ_h) are omitted. Because the point group $\mathbf{D}_{4h}$ contains $\mathbf{D}_{2d}$ as a subgroup, the S_4-axis appears as a perpendicular axis in **7**, which generates the operations S_4, $C_{2(3)}$ $(= S_4^2)$, and S_4^3. In addition, the C_4-axis appears as a perpendicular axis in **7**, which generates the operations C_4, $C_{2(3)}$ $(= C_4^2)$, and C_4^3. The C_4-axis in **7** corresponds to the $\widetilde{\mathrm{S}}_4$-axis in **6**.

3.2 Operations of $\mathbf{D}_{2d\widetilde{\sigma}\widehat{I}}$ and those of $\mathbf{D}_{4h}$

Similar examinations are conducted with respect to the operations of $\mathbf{D}_{2d\widetilde{\sigma}\widehat{I}}$ and those of the point group $\mathbf{D}_{4h}$. The resulting correspondence is summarized in Table 1. The subgroups of $\mathbf{D}_{2d\widetilde{\sigma}\widehat{I}}$ shown by Eqs. 5–9 correspond to the following subgroups of $\mathbf{D}_{4h}$:

$$\mathbf{D}_{4h} = \{\mathbf{A}, \mathbf{B}, \mathbf{C}, \mathbf{D}\} \tag{10}$$
$$\mathbf{D}_{2d} = \{\mathbf{A}, \mathbf{B}\} \tag{11}$$
$$\mathbf{D}_{4} = \{\mathbf{A}, \mathbf{C}\} \tag{12}$$
$$\mathbf{D}_{2h} = \{\mathbf{A}, \mathbf{D}\} \tag{13}$$
$$\mathbf{D}_{2} = \{\mathbf{A}\}. \tag{14}$$

The comparison between Eqs. 5–9 and 10–14 results in the following set of isomorphism: $\mathbf{D}_{4h} \cong \mathbf{D}_{2d\widetilde{\sigma}\widehat{I}}$, $\mathbf{D}_{2d} = \mathbf{D}_{2d}$ (identical), $\mathbf{D}_4 \cong \mathbf{D}_{2\widetilde{\sigma}}$, and $\mathbf{D}_{2h} \cong \mathbf{D}_{2\widehat{I}}$, and $\mathbf{D}_2 = \mathbf{D}_2$ (identical). It follows that Eqs. 1–4 for the *RS*-stereoisomeric group $\mathbf{D}_{2d\widetilde{\sigma}\widehat{I}}$ correspond respectively to the coset decompositions for the point group $\mathbf{D}_{4h}$:

$$\mathbf{D}_{4h} = \mathbf{D}_2 + \sigma_{d(1)}\mathbf{D}_2 + C'_{2(1)}\mathbf{D}_2 + \sigma_h\mathbf{D}_2 \tag{15}$$
$$\mathbf{D}_{2d} = \mathbf{D}_2 + \sigma_{d(1)}\mathbf{D}_2 \tag{16}$$
$$\mathbf{D}_{4} = \mathbf{D}_2 + C'_{2(1)}\mathbf{D}_2 \tag{17}$$
$$\mathbf{D}_{2h} = \mathbf{D}_2 + \sigma_h\mathbf{D}_2 \tag{18}$$

3.3 Factor groups derived from $\mathbf{D}_{2d\widetilde{\sigma}\widehat{I}}$ and $\mathbf{D}_{4h}$

Because the subgroup $\mathbf{D}_{2d}$ is a normal subgroup of $\mathbf{D}_{2d\widetilde{\sigma}\widehat{I}}$, Eq. 1 provides a factor group:

$$\mathbf{D}_{2d\widetilde{\sigma}\widehat{I}}/\mathbf{D}_2 = \{\mathbf{D}_2, \sigma\mathbf{D}_2, \widetilde{\sigma}\mathbf{D}_2, \widehat{I}\mathbf{D}_2\}. \tag{19}$$

As proved generally [37], a factor group generated from an *RS*-stereoisomeric group is isomorphic to the point group $\mathbf{C}_{2v}$ or the Klein four-group, so that it has exactly five subgroups, just as the point group $\mathbf{C}_{2v}$ or the Klein four-group has exactly five subgroups. The five subgroups of $\mathbf{D}_{2d\widetilde{\sigma}\widehat{I}}/\mathbf{D}_2$ are named Type I–V as follows:

$$\text{Type IV} \quad \left\{\mathbf{D}_2, \sigma\mathbf{D}_2, \widetilde{\sigma}\mathbf{D}_2, \widehat{I}\mathbf{D}_2\right\} \tag{20}$$
$$\text{Type V} \quad \left\{\mathbf{D}_2, \sigma\mathbf{D}_2\right\} \tag{21}$$
$$\text{Type II} \quad \left\{\mathbf{D}_2, \widetilde{\sigma}\mathbf{D}_2\right\} \tag{22}$$
$$\text{Type I} \quad \left\{\mathbf{D}_2, \widehat{I}\mathbf{D}_2\right\} \tag{23}$$
$$\text{Type III} \quad \left\{\mathbf{D}_2\right\} \tag{24}$$

These five types create stereoisograms of five types [37]. They are related to the coset decompositions represented by Eqs. 1–4 or by Eqs. 5–8 (along with Eq. 9).

In a parallel way, Eq. 15 provides another factor group:

$$\mathbf{D}_{4h}/\mathbf{D}_2 = \left\{\mathbf{D}_2, \sigma_{d(1)}\mathbf{D}_2, C'_{2(6)}\mathbf{D}_2, \sigma_h\mathbf{D}_2\right\} \tag{25}$$

which is isomorphic to the point group $\mathbf{C}_{2v}$ or the Klein four-group. The factor group $\mathbf{D}_{4h}/\mathbf{D}_2$ has exactly five subgroups. They are related to the coset decompositions represented by Eqs. 15–18 or by Eqs. 10–13 (along with Eq. 14).

3.4 Subgroups of $\mathbf{D}_{2d\widetilde{\sigma}\widehat{I}}$ and those of $\mathbf{D}_{4h}$

The point group $\mathbf{D}_{4h}$ has 27 subgroups up to conjugacy, which have been discussed in detail in terms of a non-redundant set of subgroups (SSG) [39]:

$$\mathrm{SSG}_{\mathbf{D}_{4h}} = \Big\{ \overset{1}{\mathbf{C}_1}, \overset{2}{\mathbf{C}_2}, \overset{3}{\mathbf{C}'_2}, \overset{4}{\mathbf{C}''_2}, \overset{5}{\mathbf{C}_s}, \overset{6}{\mathbf{C}'_s}, \overset{7}{\mathbf{C}''_s}, \overset{8}{\mathbf{C}_i}, \overset{9}{\mathbf{C}_4}, \overset{10}{\mathbf{S}_4}, \overset{11}{\mathbf{C}_{2v}}, \overset{12}{\mathbf{C}'_{2v}}, \overset{13}{\mathbf{C}''_{2v}}, \overset{14}{\mathbf{C}'''_{2v}},$$
$$\overset{15}{\mathbf{C}_{2h}}, \overset{16}{\mathbf{C}'_{2h}}, \overset{17}{\mathbf{C}''_{2h}}, \overset{18}{\mathbf{D}_2}, \overset{19}{\mathbf{D}'_2}, \overset{20}{\mathbf{C}_{4v}}, \overset{21}{\mathbf{C}_{4h}}, \overset{22}{\mathbf{D}_{2d}}, \overset{23}{\mathbf{D}'_{2d}}, \overset{24}{\mathbf{D}_{2h}}, \overset{25}{\mathbf{D}'_{2h}}, \overset{26}{\mathbf{D}_4}, \overset{27}{\mathbf{D}_{4h}} \Big\} \tag{26}$$

where the subgroups are aligned in the ascending order of their orders. For the convenience of cross reference, sequential numbers from 1 to 27 are attached to the respective subgroups. In accord with Eqs. 15–18 (and the trivial case of $\mathbf{D}_2$), the subgroups collected in Eq. 26 are categorized to give five categories, as shown in Fig. 4:

1. four subgroups of $\mathbf{D}_2$,
2. four subgroups of $\mathbf{D}_{2d}$ except those of $\mathbf{D}_2$,
3. four subgroups of $\mathbf{D}_4$ except those of $\mathbf{D}_2$,
4. eight subgroups of $\mathbf{D}_{2h}$ except those of $\mathbf{D}_2$, and
5. seven subgroups of $\mathbf{D}_{4h}$ except those of $\mathbf{D}_2$, $\mathbf{D}_{2d}$, $\mathbf{D}_4$, and $\mathbf{D}_{4h}$.

Because the *RS*-stereoisomeric group $\mathbf{D}_{2d\widetilde{\sigma}\widehat{I}}$ is isomorphic to the point group $\mathbf{D}_{4h}$, there appear 27 subgroups of $\mathbf{D}_{2d\widetilde{\sigma}\widehat{I}}$, which are respectively isomorphic to those of $\mathbf{D}_{4h}$,

$\subset \mathbf{D}_{4h}$ $\subset \mathbf{D}_{2d\widetilde{\sigma}\widehat{I}}$ (Type)	Subgroups												
	1	2	3		18								
$\mathbf{D}_2$	$\mathbf{C}_1$	$\mathbf{C}_2$	$\mathbf{C}'_2$		$\mathbf{D}_2$								
$\mathbf{D}_2$ (III)	$\mathbf{C}_1$	$\mathbf{C}_2$	$\mathbf{C}'_2$		$\mathbf{D}_2$								
		6			10	12			22				
$\mathbf{T}_d$		$\mathbf{C}'_s$			$\mathbf{S}_4$	$\mathbf{C}'_{2v}$			$\mathbf{D}_{2d}$				
$\mathbf{D}_{2d}$ (V)		$\mathbf{C}_s$			$\mathbf{S}_4$	$\mathbf{C}_{2v}$			$\mathbf{D}_{2d}$				
		4			9	19			26				
$\mathbf{D}_4$		$\mathbf{C}'_2$			$\mathbf{C}_4$	$\mathbf{D}'_2$			$\mathbf{D}_4$				
$\mathbf{D}_{2\widetilde{\sigma}}$ (II)		$\mathbf{C}_{\widetilde{\sigma}}$			$\mathbf{S}_{\widetilde{4}}$	$\mathbf{C}_{2\widetilde{\sigma}}$			$\mathbf{D}_{2\widetilde{\sigma}}$				
		5	7	8	11	13	15	16	24				
$\mathbf{D}_{2h}$		$\mathbf{C}_s$	$\mathbf{C}''_s$	$\mathbf{C}_i$	$\mathbf{C}_{2v}$	$\mathbf{C}''_{2v}$	$\mathbf{C}_{2h}$	$\mathbf{C}'_{2h}$	$\mathbf{D}_{2h}$				
$\mathbf{D}_{2\widehat{I}}$ (I)		$\mathbf{C}_{\widehat{\sigma}}$	$\mathbf{C}_{\widehat{I}}$	$\mathbf{C}_{\widehat{\sigma}'}$	$\mathbf{C}_{2\widehat{\sigma}}$	$\mathbf{C}_{2\widehat{I}}$	$\mathbf{C}'_{2\widehat{I}}$	$\mathbf{C}'_{2\widehat{\sigma}}$	$\mathbf{D}_{2\widehat{I}}$				
					14	17			20	21	23	25	27
$\mathbf{D}_{4h}$					$\mathbf{C}'''_{2v}$	$\mathbf{C}''_{2h}$			$\mathbf{C}_{4v}$	$\mathbf{C}_{4h}$	$\mathbf{D}'_{2d}$	$\mathbf{D}'_{2h}$	$\mathbf{D}_{4h}$
$\mathbf{D}_{2d\widetilde{\sigma}\widehat{I}}$ (IV)					$\mathbf{C}_{s\widetilde{\sigma}\widehat{I}}$	$\mathbf{C}_{s\widetilde{\sigma}\widehat{\sigma}}$			$\mathbf{S}_{\widetilde{4}\widehat{\sigma}}$	$\mathbf{S}_{\widetilde{4}\widehat{I}}$	$\mathbf{S}_{4\widetilde{\sigma}\widehat{\sigma}}$	$\mathbf{C}_{2v\widetilde{\sigma}\widehat{I}}$	$\mathbf{D}_{2d\widetilde{\sigma}\widehat{I}}$
order	1	2			4				8				16

Fig. 4 Subgroups of the point group $\mathbf{D}_{4h}$ and the corresponding isomorphic subgroups of the *RS*-stereoisomeric group $\mathbf{D}_{2d\widetilde{\sigma}\widehat{I}}$. For the convenience of cross reference to Eqs. 26 and 54, sequential numbers from 1 to 27 are attached to the respective subgroups. The *symbols* for the subgroups of $\mathbf{D}_{2d}$ are essentially common in both of the two isomorphic series (types III and V). The symbol for each subgroup of $\mathbf{D}_{2\widetilde{\sigma}}$ (II) contains a tilde accent. The *symbol* for each subgroup of $\mathbf{D}_{2\widehat{I}}$ (I) contains a hat accent. The *symbol* for each subgroup of $\mathbf{D}_{2d\widetilde{\sigma}\widehat{I}}$ (IV) contains both a tilde and a hat accent

as summarized in Fig. 4. By referring to the correspondence between the operations of $\mathbf{D}_{d\widetilde{\sigma}\widehat{I}}$ and those of $\mathbf{D}_{4h}$ (Table 1), the respective subgroups of $\mathbf{D}_{2d\widetilde{\sigma}\widehat{I}}$ are constructed as follows:

1. The four subgroups of the point group $\mathbf{D}_2$ are also the subgroups of the *RS*-stereoisomeric group $\mathbf{D}_{2d\widetilde{\sigma}\widehat{I}}$.

$$\mathbf{C}_1 \stackrel{1}{=} \{I\} \tag{27}$$

$$\mathbf{C}_2 \stackrel{2}{=} \{I, C_{2(3)}\} \tag{28}$$

$$\mathbf{C}'_2 \stackrel{3}{=} \{I, C_{2(1)}\} \tag{29}$$

$$\mathbf{D}_2 \stackrel{18}{=} \{I, C_{2(3)}, C_{2(1)}, C_{2(2)}\} \tag{30}$$

   The symbols of the point groups are also used to designate the subgroups of the *RS*-stereoisomeric group. See Fig. 4. These *RS*-stereoisomeric groups are categorized to type III.

2. The four subgroups of $\mathbf{D}_{2d}$ (except those of $\mathbf{D}_2$) are, at the same time, recognized as the subgroups of the *RS*-stereoisomeric group $\mathbf{D}_{2d\widetilde{\sigma}\widehat{I}}$:

$$\mathbf{C}_s \stackrel{6}{=} \{I, \sigma_{d(1)}\} \tag{31}$$

$$\mathbf{S}_4 \stackrel{10}{=} \{I, S_4, C_{2(3)}, S_4^3\} \tag{32}$$

$$\mathbf{C}_{2v} \stackrel{12}{=} \{I, C_{2(3)}, \sigma_{d(1)}, \sigma_{d(2)}\} \tag{33}$$

$$\mathbf{D}_{2d} \stackrel{22}{=} \{I, C_{2(3)}, C_{2(1)}, C_{2(2)}, \sigma_{d(1)}, \sigma_{d(2)}, S_4, S_4^3\} \tag{34}$$

The symbols of the point groups are also used to designate the subgroups of the *RS*-stereoisomeric group. The prime of the symbol $\mathbf{C}'_s$ or $\mathbf{C}'_{2v}$ ($\subset \mathbf{D}_{4h}$) is deleted to give $\mathbf{C}_s$ or $\mathbf{C}_{2v}$ in $\mathbf{D}_{2d\widetilde{\sigma}\widehat{I}}$ because of no confusion. See Fig. 4. These *RS*-stereoisomeric groups are categorized to type V.

3. The four subgroups of $\mathbf{D}_4$ (except those of $\mathbf{D}_2$) correspond to the following subgroups of $\mathbf{D}_{2\widetilde{\sigma}}$ ($-\mathbf{D}_2$).

$$\mathbf{C}_{\widetilde{\sigma}} \stackrel{4}{=} \{I, \widetilde{\sigma}_{d(1)}\} \quad (\supset \mathbf{C}_1) \tag{35}$$

$$\mathbf{S}_{\widetilde{4}} \stackrel{9}{=} \{I, \widetilde{S}_{4(3)}, C_{2(3)}, \widetilde{S}^3_{4(3)}\} \quad (\supset \mathbf{C}_2) \tag{36}$$

$$\mathbf{C}_{2\widetilde{\sigma}} \stackrel{19}{=} \{I, C_{2(3)}, \widetilde{\sigma}_{d(1)}, \widetilde{\sigma}_{d(2)}\} \quad (\supset \mathbf{C}_2) \tag{37}$$

$$\mathbf{D}_{2\widetilde{\sigma}} \stackrel{26}{=} \{I, C_{2(1)}, C_{2(2)}, C_{2(3)}, \widetilde{\sigma}_{d(1)}, \widetilde{\sigma}_{d(2)}, \widetilde{S}_{4(3)}, \widetilde{S}^3_{4(3)}\} \quad (\supset \mathbf{D}_2) \tag{38}$$

The symbols of the subgroups are selected by designating a common subgroup to $\mathbf{D}_{2d}$ (denoted in a pair of parentheses) which is attached by a suffix to refer to an uncommon operation. Each of the symbols contains a tilde accent in its suffix. For example, the symbol $\mathbf{C}_{2\widetilde{\sigma}}$ stems from the largest subgroup $\mathbf{C}_2$ (as a common subgroup to $\mathbf{D}_{2d}$) and from an uncommon operation $\widetilde{\sigma}_{d(1)}$. The symbol $\mathbf{S}_{\widetilde{4}}$ is adopted for the purpose of avoiding the confusion with $\mathbf{C}_{2\widetilde{\sigma}}$. These *RS*-stereoisomeric groups are categorized to type II.

4. The eight subgroups of $\mathbf{D}_{2h}$ (except those of $\mathbf{D}_2$) correspond to the following subgroups of $\mathbf{D}_{2\widehat{I}}$ ($-\mathbf{D}_2$).

$$\mathbf{C}_{\widehat{\sigma}} \stackrel{5}{=} \{I, \widehat{C}_{2(1)}\} \quad (\supset \mathbf{C}_1) \tag{39}$$

$$\mathbf{C}_{\widehat{I}} \stackrel{7}{=} \{I, \widehat{I}\} \quad (\supset \mathbf{C}_1) \tag{40}$$

$$\mathbf{C}'_{\widehat{\sigma}} \stackrel{8}{=} \{I, \widehat{C}_{2(3)}\} \quad (\supset \mathbf{C}_1) \tag{41}$$

$$\mathbf{C}_{2\widehat{\sigma}} \stackrel{11}{=} \{I, C_{2(3)}, \widehat{C}_{2(1)}, \widehat{C}_{2(2)}\} \quad (\supset \mathbf{C}_2) \tag{42}$$

$$\mathbf{C}_{2\widehat{I}} \stackrel{13}{=} \{I, C_{2(1)}, \widehat{C}_{2(1)}, \widehat{I}\} \quad (\supset \mathbf{C}_2) \tag{43}$$

$$\mathbf{C}'_{2\widehat{I}} \stackrel{15}{=} \{I, C_{2(3)}, \widehat{C}_{2(3)}, \widehat{I}\} \quad (\supset \mathbf{C}_2) \tag{44}$$

$$\mathbf{C}'_{2\widehat{\sigma}} \stackrel{16}{=} \{I, C_{2(1)}, \widehat{C}_{2(3)}, \widehat{C}_{2(2)}\} \quad (\supset \mathbf{C}_2) \tag{45}$$

$$\mathbf{D}_{2\widehat{I}} \stackrel{24}{=} \{I, C_{2(1)}, C_{2(2)}, C_{2(3)}, \widehat{I}, \widehat{C}_{2(1)}, \widehat{C}_{2(2)}, \widehat{C}_{2(3)}\} \quad (\supset \mathbf{D}_2) \tag{46}$$

The suffix $\widehat{\sigma}$ is used to refer to $\widehat{C}_{2(1)}$ and so on for the sake of simplicity in notations. The names of the subgroups are characterized by the symbols with a hat accent. These *RS*-stereoisomeric groups are categorized to type I.

5. The seven subgroups of $\mathbf{D}_{4h}$ (except those of $\mathbf{D}_2$, $\mathbf{D}_{2d}$, $\mathbf{D}_4$, and $\mathbf{D}_{2h}$) correspond to the following subgroups of $\mathbf{D}_{2d\widetilde{\sigma}\widehat{I}}$.

$$\mathbf{C}_{s\widetilde{\sigma}\widehat{I}} \overset{14}{=} \{I, \widetilde{\sigma}_{d(1)}, \widehat{I}, \sigma_{d(1)}\} \quad (\supset \mathbf{C}_s) \tag{47}$$

$$\mathbf{C}_{s\widetilde{\sigma}\widehat{\sigma}} \overset{17}{=} \{I, \widetilde{\sigma}_{d(1)}, \widehat{C}_{2(3)}, \sigma_{d(2)}\} \quad (\supset \mathbf{C}_s) \tag{48}$$

$$\mathbf{S}_{\widetilde{4}\widehat{\sigma}} \overset{20}{=} \{I, \widetilde{S}_{4(3)}, C_{2(3)}, \widetilde{S}^3_{4(3)}, \widehat{C}_{2(1)}, \widehat{C}_{2(2)}, \sigma_{d(1)}, \sigma_{d(2)}\} \quad (\supset \mathbf{S}_{\widetilde{4}}, \mathbf{C}_{2v}) \tag{49}$$

$$\mathbf{S}_{\widetilde{4}\widehat{I}} \overset{21}{=} \{I, \widetilde{S}_{4(3)}, C_{2(3)}, \widetilde{S}^3_{4(3)}, \widehat{I}, \widehat{C}_{2(3)}, S_{4(3)}, S^3_{4(3)}\} \quad (\supset \mathbf{S}_{\widetilde{4}}, \mathbf{S}_4) \tag{50}$$

$$\mathbf{S}_{4\widetilde{\sigma}\widehat{\sigma}} \overset{23}{=} \{I, C_{2(3)}, \widetilde{\sigma}_{d(1)}, \widetilde{\sigma}_{d(2)}, \widehat{C}_{2(1)}, \widehat{C}_{2(2)}, S_{4(3)}, S^3_{4(3)}\} \quad (\supset \mathbf{S}_4) \tag{51}$$

$$\mathbf{C}_{2v\widetilde{\sigma}\widehat{I}} \overset{25}{=} \{I, C_{2(3)}, \widetilde{\sigma}_{d(1)}, \widetilde{\sigma}_{d(2)}, \widehat{I}, \widehat{C}_{2(3)}, \sigma_{d(1)}, \sigma_{d(2)}\} \quad (\supset \mathbf{C}_{2v}) \tag{52}$$

$$\begin{aligned}\mathbf{D}_{2d\widetilde{\sigma}\widehat{I}} \overset{27}{=} \{&I, C_{2(1)}, C_{2(2)}, C_{2(3)}, \widetilde{\sigma}_{d(1)}, \widetilde{\sigma}_{d(2)}, \widetilde{S}_{4(3)}, \widetilde{S}^3_{4(3)},\\ &\widehat{I}, \widehat{C}_{2(1)}, \widehat{C}_{2(2)}, \widehat{C}_{2(3)}, \sigma_{d(1)}, \sigma_{d(6)}, S_{4(3)}, S^3_{4(3)}\} \quad (\supset \mathbf{D}_{2d})\end{aligned} \tag{53}$$

The suffix $\widehat{\sigma}$ is used to refer to $\widehat{C}_{2(1)}$ and so on for the sake of simplicity in notations. The symbol $\mathbf{S}_{\widetilde{4}\widehat{\sigma}}$ is based on the subgroup $\mathbf{S}_{\widetilde{4}}$ in place of $\mathbf{C}_{2v}$. The symbol $\mathbf{S}_{\widetilde{4}\widehat{I}}$ is based on the subgroup $\mathbf{S}_{\widetilde{4}}$ in place of $\mathbf{S}_4$. The names of the subgroups are characterized by the symbols with both a hat accent and a tilde accent. These *RS*-stereoisomeric groups are categorized to type IV.

According to the data of Fig. 4, Eq. 26 for the point group $\mathbf{D}_{4h}$ is converted into a non-redundant set of subgroups (SSG) for $\mathbf{D}_{2d\widetilde{\sigma}\widehat{I}}$:

$$\begin{aligned}\mathrm{SSG}_{\mathbf{D}_{2d\widetilde{\sigma}\widehat{I}}} = \Big\{&\overset{1}{\mathbf{C}_1}, \overset{2}{\mathbf{C}_2}, \overset{3}{\mathbf{C}'_2}, \overset{4}{\mathbf{C}_{\widetilde{\sigma}}}, \overset{5}{\mathbf{C}_{\widehat{\sigma}}}, \overset{6}{\mathbf{C}_s}, \overset{7}{\mathbf{C}_{\widehat{I}}}, \overset{8}{\mathbf{C}'_{\widehat{\sigma}}}, \overset{9}{\mathbf{S}_{\widetilde{4}}}, \overset{10}{\mathbf{S}_4}, \overset{11}{\mathbf{C}_{2\widehat{\sigma}}}, \overset{12}{\mathbf{C}_{2v}}, \overset{13}{\mathbf{C}_{2\widehat{I}}}, \overset{14}{\mathbf{C}_{s\widetilde{\sigma}\widehat{I}}}, \overset{15}{\mathbf{C}'_{2\widehat{I}}},\\ &\overset{16}{\mathbf{C}'_{2\widehat{\sigma}}}, \overset{17}{\mathbf{C}_{s\widetilde{\sigma}\widehat{\sigma}}}, \overset{18}{\mathbf{D}_2}, \overset{19}{\mathbf{C}_{2\widetilde{\sigma}}}, \overset{20}{\mathbf{S}_{\widetilde{4}\widehat{\sigma}}}, \overset{21}{\mathbf{S}_{\widetilde{4}\widehat{I}}}, \overset{22}{\mathbf{D}_{2d}}, \overset{23}{\mathbf{S}_{4\widetilde{\sigma}\widehat{\sigma}}}, \overset{24}{\mathbf{D}_{2\widehat{I}}}, \overset{25}{\mathbf{C}_{2v\widetilde{\sigma}\widehat{I}}}, \overset{26}{\mathbf{D}_{2\widetilde{\sigma}}}, \overset{27}{\mathbf{D}_{2d\widetilde{\sigma}\widehat{I}}}\Big\},\end{aligned} \tag{54}$$

where the subgroups are aligned in the ascending order of their orders. For the convenience of cross reference, sequential numbers from 1 to 27 are attached to the respective subgroups.

4 Subduction of coset representations

4.1 Coset representations

The allene skeleton **6** belongs to $\mathbf{D}_{2d}$, while the square-planar skeleton **7** belongs to $\mathbf{D}_{4h}$ from the viewpoint of the point-group theory, as shown in Fig. 3. To demonstrate the correspondence between $\mathbf{D}_{2d}$ and $\mathbf{D}_{4h}$, we focus our attention on its four midpoints (or the four edges) of 7, which are related to the four vertices of **6**.

According to the USCI approach [11], the four midpoints (or the four edges) of **7** construct an orbit governed by the coset representation $\mathbf{D}_{4h}(/\mathbf{C}'''_{2v})$ of degree 4, where the local symmetry $\mathbf{C}'''_{2v}$ is represented as follows:

$$\mathbf{C}'''_{2v} \stackrel{14}{=} \left\{I, C'_{2(1)}, \sigma_h, \sigma_{d(1)}\right\} \tag{55}$$

$$= \left\{(1)(2)(3)(4), (1)(2\,4)(3), \overline{(1)(2)(3)(4)}, \overline{(1)(2\,4)(3)}\right\}, \tag{56}$$

where a one-cycle, i.e., (1) or $\overline{(1)}$, appears in each product of cycles. Hence, the midpoint 1 is fixed under the point group $\mathbf{C}'''_{2v}$, so that the local symmetry of the midpoint 1 is determined to be $\mathbf{C}'''_{2v}$. For the coset representations of the point group $\mathbf{D}_{4h}$, see [39].

On the other hand, the four vertices of the allene skeleton **6** (Fig. 3) construct an orbit, which is governed by the coset representation $\mathbf{D}_{2d\widetilde{\sigma}\widehat{I}}(/\mathbf{C}_{s\widetilde{\sigma}\widehat{I}})$ of degree $|\mathbf{D}_{2d\widetilde{\sigma}\widehat{I}}|/|\mathbf{C}_{s\widetilde{\sigma}\widehat{I}}|$ $(= 16/4 = 4)$. The coset representation $\mathbf{D}_{2d\widetilde{\sigma}\widehat{I}}(/\mathbf{C}_{s\widetilde{\sigma}\widehat{I}})$ consists of the same set of products of cycles as $\mathbf{D}_{4h}(/\mathbf{C}'''_{2v})$ (Table 1). The local symmetry $\mathbf{C}_{s\widetilde{\sigma}\widehat{I}}$ (Eq. 47) is isomorphic to $\mathbf{C}'''_{2v}$ (Eq. 56):

$$\mathbf{C}_{s\widetilde{\sigma}\widehat{I}} \stackrel{14}{=} \left\{I, \widetilde{\sigma}_{d(1)}, \widehat{I}, \sigma_{d(1)}\right\}$$

$$= \left\{(1)(2)(3)(4), (1)(2\,4)(3), \overline{(1)(2)(3)(4)}, \overline{(1)(2\,4)(3)}\right\}, \tag{57}$$

which contains the same set of products of cycles as contained in Eq. 56. Because a one-cycle, i.e., (1) or $\overline{(1)}$, appears in each product of cycles, the vertex 1 is fixed under the point group $\mathbf{C}_{s\widetilde{\sigma}\widehat{I}}$, so that the local symmetry of the vertex 1 is determined to be $\mathbf{C}_{s\widetilde{\sigma}\widehat{I}}$.

4.2 Subduction of coset representations and USCI-CFs for point groups

The subduction of the coset representation $\mathbf{D}_{4h}(/\mathbf{C}'''_{2v})$ is conducted according to the USCI approach [11]. For example, the $\mathbf{D}_{4h}(/\mathbf{C}'''_{2v})$-orbit is restricted to $\mathbf{D}_{2d}$ in accord with the subduction of the coset representation:

$$\mathbf{D}_{4h}\left(/\mathbf{C}'''_{2v}\right) \downarrow \mathbf{D}_{2d} = \mathbf{D}_{2d}\left(/\mathbf{C}_{s}\right), \tag{58}$$

which is listed in the 22nd row of Table 2. Note that the degree of $\mathbf{D}_{2d}(/\mathbf{C}_s)$ is calculated to be $|\mathbf{D}_{2d}|/|\mathbf{C}_s| = 8/2 = 4$. Hence, the $\mathbf{D}_{4h}(/\mathbf{C}'''_{2v})$-orbit of the four midpoints of **7** is not separated under this subduction so as to retain one orbit governed by the coset representation $\mathbf{D}_{2d}(/\mathbf{C}_s)$.

The procedure for subduction is repeated to cover all of the SSG (Eq. 26) to give the data summarized in the subduction column of Table 2. For a related subduction of another coset representation $\mathbf{D}_{4h}(/\mathbf{C}'''_{2v})$, see [39].

Each coset representation generated by the subduction is characterized by a sphericity index (SI), i.e., a_d for a homospheric coset representation of degree d, c_d for a enantiospheric coset representation of degree d, and b_d for a hemispheric coset representation of degree d. Because the whole result of the subduction is characterized

Table 2 Subduction of $\mathbf{D}_{4h}(/\mathbf{C}'''_{2v})$

	Subgroup ($\downarrow \mathbf{G}_j$)	Subduction ($\mathbf{D}_{4h}(/\mathbf{C}'''_{2v}) \downarrow \mathbf{G}_j$)	USCI-CF	USCI	GEM		
					Total ($\widehat{N}_j$)	Chiral ($\widehat{N}_j^{(e)}$)	Achiral ($\widehat{N}_j^{(a)}$)
1	$\mathbf{C}_1$	$4\mathbf{C}_1(/\mathbf{C}_1)$	b_1^4	s_1^4	1/16	1/16	0
2	$\mathbf{C}_2$	$2\mathbf{C}_2(/\mathbf{C}_1)$	b_2^2	s_2^2	1/16	1/16	0
3	$\mathbf{C}'_2$	$2\mathbf{C}'_2(/\mathbf{C}_1)$	b_2^2	s_2^2	1/8	1/8	0
4	$\mathbf{C}''_2$	$\mathbf{C}''_2(/\mathbf{C}_1) + 2\mathbf{C}''_2(/\mathbf{C}_2)$	$b_1^2 b_2$	$s_1^2 s_2$	1/8	1/8	0
5	$\mathbf{C}_s$	$2\mathbf{C}_s(/\mathbf{C}_1)$	c_2^2	s_2^2	1/8	$-1/8$	1/4
6	$\mathbf{C}'_s$	$\mathbf{C}'_s(/\mathbf{C}_1) + 2\mathbf{C}'_s(/\mathbf{C}_s)$	$a_1^2 c_2$	$s_1^2 s_2$	1/8	$-1/8$	1/4
7	$\mathbf{C}''_s$	$4\mathbf{C}''_s(/\mathbf{C}_s)$	a_1^4	a_1^4	1/16	$-1/16$	1/8
8	$\mathbf{C}_i$	$2\mathbf{C}_i(/\mathbf{C}_1)$	c_2^2	s_2^2	1/16	$-1/16$	1/8
9	$\mathbf{C}_4$	$\mathbf{C}_4(/\mathbf{C}_1)$	b_4	s_4	1/8	1/8	0
10	$\mathbf{S}_4$	$\mathbf{S}_4(/\mathbf{C}_1)$	c_4	s_4	1/8	$-1/8$	1/4
11	$\mathbf{C}_{2v}$	$\mathbf{C}_{2v}(/\mathbf{C}_1)$	c_4	s_4	0	0	0
12	$\mathbf{C}'_{2v}$	$\mathbf{C}'_{2v}(/\mathbf{C}_s) + \mathbf{C}'_{2v}(/\mathbf{C}'_s)$	a_2^2	s_2^2	0	0	0
13	$\mathbf{C}''_{2v}$	$2\mathbf{C}''_{2v}(/\mathbf{C}'_s)$	a_2^2	s_2^2	0	0	0
14	$\mathbf{C}'''_{2v}$	$\mathbf{C}'''_{2v}(/\mathbf{C}'_s) + 2\mathbf{C}'''_{2v}(/\mathbf{C}_{2v})$	$a_1^2 a_2$	$s_1^2 s_2$	0	0	0
15	$\mathbf{C}_{2h}$	$2\mathbf{C}_{2h}(/\mathbf{C}_s)$	a_2^2	s_2^2	0	0	0
16	$\mathbf{C}'_{2h}$	$\mathbf{C}'_{2h}(/\mathbf{C}_1)$	c_4	s_4	0	0	0
17	$\mathbf{C}''_{2h}$	$\mathbf{C}''_{2h}(/\mathbf{C}_2) + \mathbf{C}''_{2h}(/\mathbf{C}_s)$	$a_2 c_2$	s_2^2	0	0	0
18	$\mathbf{D}_2$	$\mathbf{D}_2(/\mathbf{C}_1)$	b_4	s_4	0	0	0
19	$\mathbf{D}'_2$	$\mathbf{D}'_2(/\mathbf{C}'_2) + \mathbf{D}'_2(/\mathbf{C}''_2)$	b_2^2	s_2^2	0	0	0
20	$\mathbf{C}_{4v}$	$\mathbf{C}_{4v}(/\mathbf{C}'_s)$	a_4	s_4	0	0	0
21	$\mathbf{C}_{4h}$	$\mathbf{C}_{4h}(/\mathbf{C}_s)$	a_4	s_4	0	0	0
22	$\mathbf{D}_{2d}$	$\mathbf{D}_{2d}(/\mathbf{C}_s)$	a_4	s_4	0	0	0
23	$\mathbf{D}'_{2d}$	$\mathbf{D}'_{2d}(/\mathbf{C}'_2)$	c_4	s_4	0	0	0
24	$\mathbf{D}_{2h}$	$\mathbf{D}_{2h}(/\mathbf{C}''_s)$	a_4	s_4	0	0	0
25	$\mathbf{D}'_{2h}$	$\mathbf{D}'_{2h}(/\mathbf{C}'_{2h}) + \mathbf{D}'_{2h}(/\mathbf{C}''_{2h})$	a_2^2	s_2^2	0	0	0
26	$\mathbf{D}_4$	$\mathbf{D}_4(/\mathbf{C}''_2)$	b_4	s_4	0	0	0
27	$\mathbf{D}_{4h}$	$\mathbf{D}_{4h}(/\mathbf{C}'''_{2v})$	a_4	s_4	0	0	0

by a product of SIs, the product of SIs is called a unit subduced cycle index with chirality fittingness (USCI-CF) according to Def. 9.3 of [11]. For example, the subduction $\mathbf{D}_{4h}(/\mathbf{C}'''_{2v}) \downarrow \mathbf{D}_{2d}$ (Eq. 58) is characterized by a USCI-CF a_4. Similarly, the data collected in the subduction column of Table 2 provide USCI-CFs collected in the USCI-CF column of the same table. When sphericities are not taken into consideration, USCIs (without chirality fittingness) are obtained by putting $s_d = a_d = b_d = c_d$ according to Def. 9.2 of [11], as collected in the USCI column of Table 2. By obeying the procedure exemplified by Table 2, we are able to obtain the full list of the USCI-CFs of $\mathbf{D}_{4h}$.

4.3 Subduction of coset representations and USCI-CFs for *RS*-stereoisomeric groups

4.3.1 Subduction to point subgroups

Because the *RS*-Stereoisomeric group $\mathbf{D}_{2d\widetilde{\sigma}\widehat{I}}$ contains the point group $\mathbf{D}_{2d}$ as a subgroup, the subduction of $\mathbf{D}_{2d\widetilde{\sigma}\widehat{I}}(/\mathbf{C}_{s\widetilde{\sigma}\widehat{I}})$ to the point group $\mathbf{D}_{2d}$ or its subgroup can be treated in a similar way to the coset representation $\mathbf{D}_{4h}(/\mathbf{C}'''_{2v})$. For example, the $\mathbf{D}_{2d\widetilde{\sigma}\widehat{I}}(/\mathbf{C}_{s\widetilde{\sigma}\widehat{I}})$-orbit is restricted to $\mathbf{D}_{2d}$ in accord with the subduction of the coset representation:

$$\mathbf{D}_{2d\widetilde{\sigma}\widehat{I}}\left(/\mathbf{C}_{s\widetilde{\sigma}\widehat{I}}\right) \downarrow \mathbf{D}_{2d} = \mathbf{D}_{2d}\left(/\mathbf{C}_{s}\right), \tag{59}$$

which is shown in the 22nd row of Table 3. Note that the degree of $\mathbf{D}_{2d}(/\mathbf{C}_s)$ (homospheric) is calculated to be $|\mathbf{D}_{2d}|/|\mathbf{C}_s| = 8/2 = 4$. This means that the $\mathbf{D}_{2d\widetilde{\sigma}\widehat{I}}(/\mathbf{C}_{s\widetilde{\sigma}\widehat{I}})$-orbit of the four vertices of **6** is not separated under this subduction so as to retain one orbit governed by the coset representation $\mathbf{D}_{2d}(/\mathbf{C}_s)$. Because the right-hand side of Eq. 59 is concerned with the point group $\mathbf{D}_{2d}$, the subduction $\mathbf{D}_{d\widetilde{\sigma}\widehat{I}}(/\mathbf{C}_{s\widetilde{\sigma}\widehat{I}}) \downarrow \mathbf{D}_{2d}$ is characterized by a USCI-CF, a_4.

Because the subgroup $\mathbf{C}'_s$ of $\mathbf{D}_{4h}$ is identical with the subgroup $\mathbf{C}_s$ of $\mathbf{D}_{2d\widetilde{\sigma}\widehat{I}}$, the subduction to $\mathbf{C}_s$ is shown as follows:

$$\mathbf{D}_{d\widetilde{\sigma}\widehat{I}}\left(/\mathbf{C}_{s\widetilde{\sigma}\widehat{I}}\right) \downarrow \mathbf{C}_s = \mathbf{C}_s\left(/\mathbf{C}_1\right) + 2\mathbf{C}_s\left(/\mathbf{C}_s\right) \tag{60}$$

which appears in the 6-th row of Table 3. The degree of $\mathbf{C}_s(/\mathbf{C}_1)$ (enantiospheric) is equal to $|\mathbf{C}_s|/|\mathbf{C}_1| = 2/1 = 2$, while the degree of $\mathbf{C}_s(/\mathbf{C}_s)$ (homospheric) is equal to $|\mathbf{C}_s|/|\mathbf{C}_s| = 2/2 = 1$. Hence, the subduction $\mathbf{D}_{2d\widetilde{\sigma}\widehat{I}}(/\mathbf{C}_{s\widetilde{\sigma}\widehat{I}}) \downarrow \mathbf{C}_s$ is characterized by a USCI-CF, $a_1^2 c_2$.

The subductions to the subgroups collected in the $\mathbf{D}_{2d}$(V)-row of Fig. 4 (i.e., $\mathbf{C}_s$, $\mathbf{S}_4$, $\mathbf{C}_{2v}$, and $\mathbf{D}_{2d}$) and those collected in the $\mathbf{D}_2$(III)-row (i.e., $\mathbf{C}_1$, $\mathbf{C}_2$, $\mathbf{C}'_2$, and $\mathbf{D}_2$) can be discussed in a parallel way, so that the corresponding subduction results and USCI-CFs collected in Table 3 are equivalent to the counterparts collected in Table 2.

4.3.2 Subduction to RS-stereoisomeric subgroups

In order to extend the concept of sphericities under point groups [11] to the concept of sphericities under *RS*-stereoisomeric groups, an *RS*-stereoisomeric group and its subgroups (also *RS*-stereoisomeric groups) are categorized by means of extended chirality/achirality:

1. If an *RS*-stereoisomeric group contains a (roto)reflection operation and/or a ligand reflection operation (with a hat accent in the present notation), it is defined to be ex-achiral.
2. If an *RS*-stereoisomeric group contains no (roto)reflection operations nor ligand reflection operations, it is defined to be ex-chiral.

Table 3 Subduction of $\mathbf{D}_{2d\widetilde{\sigma}\widehat{I}}(/\mathbf{C}_{s\widetilde{\sigma}\widehat{I}})$

	Subgroup ($\downarrow \acute{\mathbf{G}}_j$ type)	Subduction ($\mathbf{D}_{2d\widetilde{\sigma}\widehat{I}}(/\mathbf{C}_{s\widetilde{\sigma}\widehat{I}}) \downarrow \acute{\mathbf{G}}_j$)	USCI-CF	USCI	TEM					
					$\widehat{N}_j$	$\widehat{N}_j^{(I)}$	$\widehat{N}_j^{(II)}$	$\widehat{N}_j^{(III)}$	$\widehat{N}_j^{(IV)}$	$\widehat{N}_j^{(V)}$
1	$\mathbf{C}_1$ III	$4\mathbf{C}_1(/\mathbf{C}_1)$	b_1^4	s_1^4	1/16	0	0	1/16	0	0
2	$\mathbf{C}_2$ III	$2\mathbf{C}_2(/\mathbf{C}_1)$	b_2^2	s_2^2	1/16	0	0	1/16	0	0
3	$\mathbf{C}'_2$ III	$2\mathbf{C}'_2(/\mathbf{C}_1)$	b_2^2	s_2^2	1/8	0	0	1/8	0	0
4	$\mathbf{C}_{\widetilde{\sigma}}$ II	$\mathbf{C}_{\widetilde{\sigma}}(/\mathbf{C}_1) + 2\mathbf{C}_{\widetilde{\sigma}}(/\mathbf{C}_{\widetilde{\sigma}})$	$b_1^2 b_2$	$s_1^2 s_2$	1/8	0	1/4	−1/8	0	0
5	$\mathbf{C}_{\widehat{\sigma}}$ I	$2\mathbf{C}_{\widehat{\sigma}}(/\mathbf{C}_1)$	c_2^2	s_2^2	1/8	1/4	0	−1/8	0	0
6	$\mathbf{C}_s$ V	$\mathbf{C}_s(/\mathbf{C}_1) + 2\mathbf{C}_s(/\mathbf{C}_s)$	$a_1^2 c_2$	$s_1^2 s_2$	1/8	0	0	−1/8	0	1/4
7	$\mathbf{C}_{\widehat{I}}$ I	$4\mathbf{C}_{\widehat{I}}(/\mathbf{C}_{\widehat{I}})$	a_1^4	a_1^4	1/16	1/8	0	−1/16	0	0
8	$\mathbf{C}'_{\widehat{\sigma}}$ I	$2\mathbf{C}'_{\widehat{\sigma}}(/\mathbf{C}_1)$	c_2^2	s_2^2	1/16	1/8	0	−1/16	0	0
9	$\mathbf{S}_{\widetilde{4}}$ II	$\mathbf{S}_{\widetilde{4}}(/\mathbf{C}_1)$	b_4	s_4	1/8	0	1/4	−1/8	0	0
10	$\mathbf{S}_4$ V	$\mathbf{S}_4(/\mathbf{C}_1)$	c_4	s_4	1/8	0	0	−1/8	0	1/4
11	$\mathbf{C}_{2\widehat{\sigma}}$ I	$\mathbf{C}_{2\widehat{\sigma}}(/\mathbf{C}_1)$	c_4	s_4	0	0	0	0	0	0
12	$\mathbf{C}_{2v}$ V	$\mathbf{C}_{2v}(/\mathbf{C}_s) + \mathbf{C}_{2v}(/\mathbf{C}'_s)$	a_2^2	s_2^2	0	0	0	0	0	0
13	$\mathbf{C}_{2\widehat{I}}$ I	$2\mathbf{C}_{2\widehat{I}}(/\mathbf{C}_{\widehat{I}})$	a_2^2	s_2^2	0	0	0	0	0	0
14	$\mathbf{C}_{s\widetilde{\sigma}\widehat{I}}$ IV	$\mathbf{C}_{s\widetilde{\sigma}\widehat{I}}(/\mathbf{C}_{\widehat{I}}) + 2\mathbf{C}_{s\widetilde{\sigma}\widehat{I}}(/\mathbf{C}_{s\widetilde{\sigma}\widehat{I}})$	$a_1^2 a_2$	$s_1^2 s_2$	0	−1/4	−1/4	1/4	1/2	−1/4
15	$\mathbf{C}'_{2\widehat{I}}$ I	$2\mathbf{C}'_{2\widehat{I}}(/\mathbf{C}_{\widehat{I}})$	a_2^2	s_2^2	0	0	0	0	0	0
16	$\mathbf{C}'_{2\widehat{\sigma}}$ I	$\mathbf{C}'_{2\widehat{\sigma}}(/\mathbf{C}_1)$	c_4	s_4	0	0	0	0	0	0
17	$\mathbf{C}_{s\widetilde{\sigma}\widehat{\sigma}}$ IV	$\mathbf{C}_{s\widetilde{\sigma}\widehat{\sigma}}(/\mathbf{C}_{\widetilde{\sigma}}) + \mathbf{C}_{s\widetilde{\sigma}\widehat{\sigma}}(/\mathbf{C}_s)$	$a_2 c_2$	s_2^2	0	−1/4	−1/4	1/4	1/2	−1/4
18	$\mathbf{D}_2$ III	$\mathbf{D}_2(/\mathbf{C}_1)$	b_4	s_4	0	0	0	0	0	0
19	$\mathbf{C}_{2\widetilde{\sigma}}$ II	$\mathbf{C}_{2\widetilde{\sigma}}(/\mathbf{C}_{\widetilde{\sigma}}) + \mathbf{C}_{2\widetilde{\sigma}}(/\mathbf{C}'_{\widetilde{\sigma}})$	b_2^2	s_2^2	0	0	0	0	0	0
20	$\mathbf{S}_{\widetilde{4}\widehat{\sigma}}$ IV	$\mathbf{S}_{\widetilde{4}\widehat{\sigma}}(/\mathbf{C}_s)$	a_4	s_4	0	−1/4	−1/4	1/4	1/2	−1/4
21	$\mathbf{S}_{\widetilde{4}\widehat{I}}$ IV	$\mathbf{S}_{\widetilde{4}\widehat{I}}(/\mathbf{C}_{\widehat{I}})$	a_4	s_4	0	−1/4	−1/4	1/4	1/2	−1/4
22	$\mathbf{D}_{2d}$ V	$\mathbf{D}_{2d}(/\mathbf{C}_s)$	a_4	s_4	0	0	0	0	0	0
23	$\mathbf{S}_{4\widetilde{\sigma}\widehat{\sigma}}$ IV	$\mathbf{S}_{4\widetilde{\sigma}\widehat{\sigma}}(/\mathbf{C}_{\widetilde{\sigma}})$	c_4	s_4	0	−1/4	−1/4	1/4	1/2	−1/4
24	$\mathbf{D}_{2\widehat{I}}$ I	$\mathbf{D}_{2\widehat{I}}(/\mathbf{C}_{\widehat{I}})$	a_4	s_4	0	0	0	0	0	0
25	$\mathbf{C}_{2v\widetilde{\sigma}\widehat{I}}$ IV	$\mathbf{C}_{2v\widetilde{\sigma}\widehat{I}}(/\mathbf{C}_{s\widetilde{\sigma}\widehat{I}}) + \mathbf{C}_{2v\widetilde{\sigma}\widehat{I}}(/\mathbf{C}'_{s\widetilde{\sigma}\widehat{I}})$	a_2^2	s_2^2	0	1/4	1/4	−1/4	−1/2	1/4
26	$\mathbf{D}_{2\widetilde{\sigma}}$ II	$\mathbf{D}_{2\widetilde{\sigma}}(/\mathbf{C}_{\widetilde{\sigma}})$	b_4	s_4	0	0	0	0	0	0
27	$\mathbf{D}_{2d\widetilde{\sigma}\widehat{I}}$ IV	$\mathbf{D}_{2d\widetilde{\sigma}\widehat{I}}(/\mathbf{C}_{s\widetilde{\sigma}\widehat{I}})$	a_4	s_4	0	1/2	1/2	−1/2	−1	1/2

Note that the prefix ‘ex’ is an abbreviated form of ‘extended’.

Among the 27 subgroups of the *RS*-stereoisomeric group $\mathbf{D}_{2d\widetilde{\sigma}\widehat{I}}$ listed in Eq. 54, those listed as type II and type III in Fig. 4 are ex-chiral according to the definition described in the preceding paragraph. On the other hand, those listed as type I, type IV, and type V are determined to be ex-achiral.

It should be noted that type-I subgroups of the *RS*-stereoisomeric group $\mathbf{D}_{2d\widetilde{\sigma}\widehat{I}}$ (cf. $\mathbf{D}_{2\widehat{I}}$(I)-row of Table 4) are ex-achiral, while the corresponding subgroups of the point group $\mathbf{D}_{2d}$ are (ex-)chiral. Thus, the correspondence between the (ex-)chiral subgroups of $\mathbf{D}_{2d}$ and the ex-achiral type-I subgroups of $\mathbf{D}_{2d\widetilde{\sigma}\widehat{I}}$ is as follows: $\mathbf{C}_1$ vs. $\mathbf{C}_{\widehat{\sigma}}$; $\mathbf{C}_1$ vs. $\mathbf{C}_{\widehat{I}}$; $\mathbf{C}_1$ vs. $\mathbf{C}_{\widehat{\sigma}'}$; $\mathbf{C}_2$ vs. $\mathbf{C}_{2\widehat{\sigma}}$; $\mathbf{C}_2$ vs. $\mathbf{C}_{2\widehat{I}}$; $\mathbf{C}_2$ vs. $\mathbf{C}'_{2\widehat{I}}$; $\mathbf{C}'_2$ vs. $\mathbf{C}'_{2\widehat{\sigma}}$; and $\mathbf{D}_2$ vs. $\mathbf{D}_{2\widehat{I}}$. This correspondence reflects self-holantimeric relationships (due to asclerality), which are inherent in type-I stereoisograms. Discussions based on the point group $\mathbf{D}_{2d}$ would overlook this type of hidden properties.

A coset representation $\acute{\mathbf{G}}(/\acute{\mathbf{G}}_i)$ based on an *RS*-stereoisomeric group $\acute{\mathbf{G}}$ is categorized as follows:

1. If both the *RS*-stereoisomeric groups, $\acute{\mathbf{G}}$ (global symmetry) and $\acute{\mathbf{G}}_i$ (local symmetry), are ex-achiral, the coset representation $\acute{\mathbf{G}}(/\acute{\mathbf{G}}_i)$ is defined as being homospheric and characterized by a sphericity index a_d where $d = |\acute{\mathbf{G}}|/|\acute{\mathbf{G}}_i|$.
2. If the global *RS*-stereoisomeric group $\acute{\mathbf{G}}$ is ex-achiral and the local *RS*-stereoisomeric group $\acute{\mathbf{G}}_i$) is ex-chiral, the coset representation $\acute{\mathbf{G}}(/\acute{\mathbf{G}}_i)$ is defined as being enantiospheric and characterized by a sphericity index c_d where $d = |\acute{\mathbf{G}}|/|\acute{\mathbf{G}}_i|$.
3. If both the *RS*-stereoisomeric groups, $\acute{\mathbf{G}}$ (global symmetry) and $\acute{\mathbf{G}}_i$) (local symmetry), are ex-chiral, the coset representation $\acute{\mathbf{G}}(/\acute{\mathbf{G}}_i)$ is defined as being hemispheric and characterized by a sphericity index b_d where $d = |\acute{\mathbf{G}}|/|\acute{\mathbf{G}}_i|$.

A coset representation $\acute{\mathbf{G}}(/\acute{\mathbf{G}}_i)$ is subduced into a subgroup $\acute{\mathbf{G}}_j$. The subduction $\acute{\mathbf{G}}(/\acute{\mathbf{G}}_i) \downarrow \acute{\mathbf{G}}_j$ is represented by a sum of coset representations based on the subgroup $\acute{\mathbf{G}}_j$. The sum of coset representations is characterized by a product of sphericity indices, which is also called *a unit subduced cycle index with chirality fittingness* (USCI-CF).

The subductions of $\mathbf{D}_{2d\widetilde{\sigma}\widehat{I}}(/\mathbf{C}_{s\widetilde{\sigma}\widehat{I}})$ to respective subgroups shown in Eq. 54 are listed in the subduction column of Table 3. The corresponding USCI-CFs are collected in the USCI-CF column of Table 3.

For example, the subduction of $\mathbf{D}_{2d\widetilde{\sigma}\widehat{I}}(/\mathbf{C}_{s\widetilde{\sigma}\widehat{I}})$ to $\mathbf{C}_{\widehat{\sigma}}$ is represented as follows:

$$\mathbf{D}_{2d\widetilde{\sigma}\widehat{I}}(/\mathbf{C}_{s\widetilde{\sigma}\widehat{I}}) \downarrow \mathbf{C}_{\widehat{\sigma}} = 2\mathbf{C}_{\widehat{\sigma}}(/\mathbf{C}_1), \tag{61}$$

where the degree of the coset representation $\mathbf{C}_{\widehat{\sigma}}(/\mathbf{C}_1)$ is calculated to be $|\mathbf{C}_{\widehat{\sigma}}|/|\mathbf{C}_1| = 2/1 = 2$. Because the subgroup $\mathbf{C}_{\widehat{\sigma}}$ is presumed to be ex-achiral and $\mathbf{C}_1$ is ex-chiral, the the coset representation $\mathbf{C}_{\widehat{\sigma}}(/\mathbf{C}_1)$ is concluded to be enantiospheric. Hence, this subduction gives the USCI-CF c_2^2 by considering the sphericities of the respective coset representations, as listed in the 5th row of Table 3. This behavior corresponds to the subduction $\mathbf{D}_{4h}(/\mathbf{C}'''_{2v}) \downarrow \mathbf{C}_s$ shown in the 5th row of Table 2.

Another example is the subduction of $\mathbf{D}_{2d\widetilde{\sigma}\widehat{I}}(/\mathbf{C}_{s\widetilde{\sigma}\widehat{I}})$ to $\mathbf{C}_{s\widetilde{\sigma}\widehat{\sigma}}$ as follows:

$$\mathbf{D}_{2d\widetilde{\sigma}\widehat{I}}(/\mathbf{C}_{s\widetilde{\sigma}\widehat{I}}) \downarrow \mathbf{C}_{s\widetilde{\sigma}\widehat{\sigma}} = \mathbf{C}_{s\widetilde{\sigma}\widehat{\sigma}}(/\mathbf{C}_{\widetilde{\sigma}}) + \mathbf{C}_{s\widetilde{\sigma}\widehat{\sigma}}(/\mathbf{C}_s), \tag{62}$$

which is shown at the 17th row of Table 3. This subduction gives the USCI-CF a_2c_2 by considering the sphericities of the respective coset representations. This behavior corresponds to the subduction $\mathbf{D}_{4h}(/\mathbf{C}'''_{2v}) \downarrow \mathbf{C}''_{2h}$ shown in the 17th row of Table 2.

5 Symmetry-itemized enumeration

5.1 Fixed-point vectors for symmetry-itemized enumeration

A subduced cycle index with chirality fittingness (SCI-CF) defined as a product of USCI-CFs (Def. 19.3 of [11]) is capable of evaluating the number of fixed promolecules as *RS*-stereoisomers. Such an SCI-CF is identical with the corresponding USCI-CF (the USCI-CF-column of Table 3) in the present enumeration of quadruplets of *RS*-stereoisomers, because there exists a single orbit.

Suppose that substituents for the four positions of **1** (Fig. 1) are selected from an inventory of proligands:

$$\mathbf{X} = \left\{\mathrm{A, B, X, Y};\quad \mathrm{p, q, r, s};\quad \overline{\mathrm{p}}, \overline{\mathrm{q}}, \overline{\mathrm{r}}, \overline{\mathrm{s}}\right\}, \tag{63}$$

where the letters A, B, X, and Y represent achiral proligands and the pairs of p/$\overline{\mathrm{p}}$, q/$\overline{\mathrm{q}}$, r/$\overline{\mathrm{r}}$, and s/$\overline{\mathrm{s}}$ represent pairs of enantiomeric proligands in isolation (when detached). According to Lemma 19.2 of [11], we use the following ligand-inventory functions:

$$a_d = \mathrm{A}^d + \mathrm{B}^d + \mathrm{X}^d + \mathrm{Y}^d \tag{64}$$

$$c_d = \mathrm{A}^d + \mathrm{B}^d + \mathrm{X}^d + \mathrm{Y}^d + 2\mathrm{p}^{d/2}\overline{\mathrm{p}}^{d/2} + 2\mathrm{q}^{d/2}\overline{\mathrm{q}}^{d/2} + 2\mathrm{r}^{d/2}\overline{\mathrm{r}}^{d/2} + 2\mathrm{s}^{d/2}\overline{\mathrm{s}}^{d/2} \tag{65}$$

$$b_d = \mathrm{A}^d + \mathrm{B}^d + \mathrm{X}^d + \mathrm{Y}^d + \mathrm{p}^d + \mathrm{q}^d + \mathrm{r}^d + \mathrm{s}^d + \overline{\mathrm{p}}^d + \overline{\mathrm{q}}^d + \overline{\mathrm{r}}^d + \overline{\mathrm{s}}^d. \tag{66}$$

It should be noted that the power $d/2$ appearing in Eq. 65 is an integer because the subscript d of c_d is always even in the light of the enantiosphericity of the corresponding orbit. These ligand-inventory functions are introduced into an SCI-CF to give a generating function, in which the coefficient of the term $\mathrm{A}^a\mathrm{B}^b\mathrm{X}^x\mathrm{Y}^y\mathrm{p}^p\overline{\mathrm{p}}^{\overline{p}}\mathrm{q}^q\overline{\mathrm{q}}^{\overline{q}}\mathrm{r}^r\overline{\mathrm{q}}^{\overline{r}}\mathrm{s}^s\overline{\mathrm{q}}^{\overline{s}}$ indicates the number of fixed promolecules to be counted. Because A, B, etc. appear symmetrically, the term can be represented by the following partition:

$$[\theta] = [a, b, x, y;\, p, \overline{p}, q, \overline{q}, r, \overline{r}, s, \overline{s}]\,, \tag{67}$$

where we put $a \geq b \geq x \geq y$, $p \geq \overline{p}$, $q \geq \overline{q}$, $r \geq \overline{r}$, $s \geq \overline{s}$, and $p \geq q \geq r \geq s$ without losing generality. For the purpose of systematic enumeration of allenes, the following partitions are taken into consideration, where partitions with achiral and chiral proligands are listed:

$$[\theta]_1 = [4, 0, 0, 0; 0, 0, 0, 0, 0, 0, 0, 0] \quad \left(\text{for } \mathrm{A}^4\text{etc.}\right) \tag{68}$$

$$[\theta]_2 = [3, 1, 0, 0; 0, 0, 0, 0, 0, 0, 0, 0] \quad \left(\text{for } \mathrm{A}^3\mathrm{B} \text{ etc.}\right) \tag{69}$$

$$[\theta]_3 = [3, 0, 0, 0; 1, 0, 0, 0, 0, 0, 0, 0] \quad \left(\text{for } \mathrm{A}^3\mathrm{p} \text{ etc.}\right) \tag{70}$$

$$[\theta]_4 = [2, 2, 0, 0; 0, 0, 0, 0, 0, 0, 0, 0] \quad \left(\text{for } \mathrm{A}^2B^2\text{etc.}\right) \tag{71}$$

$$[\theta]_5 = [2, 0, 0, 0; 2, 0, 0, 0, 0, 0, 0, 0] \quad \left(\text{for A}^2 p^2 \text{etc.}\right) \tag{72}$$

$$[\theta]_6 = [2, 1, 1, 0; 0, 0, 0, 0, 0, 0, 0, 0] \quad \left(\text{for A}^2\text{BX etc.}\right) \tag{73}$$

$$[\theta]_7 = [2, 1, 0, 0; 1, 0, 0, 0, 0, 0, 0, 0] \quad \left(\text{for A}^2\text{Bp etc.}\right) \tag{74}$$

$$[\theta]_8 = [2, 0, 0, 0; 1, 1, 0, 0, 0, 0, 0, 0] \quad \left(\text{for A}^2\text{p}\overline{\text{p}}\text{etc.}\right) \tag{75}$$

$$[\theta]_9 = [2, 0, 0, 0; 1, 0, 1, 0, 0, 0, 0, 0] \quad \left(\text{for A}^2\text{pq etc.}\right) \tag{76}$$

$$[\theta]_{10} = [1, 1, 1, 1; 0, 0, 0, 0, 0, 0, 0, 0] \quad \left(\text{for ABXY}\right) \tag{77}$$

$$[\theta]_{11} = [1, 1, 1, 0; 1, 0, 0, 0, 0, 0, 0, 0] \quad \left(\text{for ABXp etc.}\right) \tag{78}$$

$$[\theta]_{12} = [1, 1, 0, 0; 2, 0, 0, 0, 0, 0, 0, 0] \quad \left(\text{for ABp}^2\text{etc.}\right) \tag{79}$$

$$[\theta]_{13} = [1, 1, 0, 0; 1, 1, 0, 0, 0, 0, 0, 0] \quad \left(\text{for ABp}\overline{\text{p}}\text{etc.}\right) \tag{80}$$

$$[\theta]_{14} = [1, 1, 0, 0; 1, 0, 1, 0, 0, 0, 0, 0] \quad \left(\text{for ABpq etc.}\right) \tag{81}$$

$$[\theta]_{15} = [1, 0, 0, 0; 3, 0, 0, 0, 0, 0, 0, 0] \quad \left(\text{for Ap}^3\text{etc.}\right) \tag{82}$$

$$[\theta]_{16} = [1, 0, 0, 0; 2, 1, 0, 0, 0, 0, 0, 0] \quad \left(\text{for Ap}^2\overline{\text{p}}\text{etc.}\right) \tag{83}$$

$$[\theta]_{17} = [1, 0, 0, 0; 2, 0, 1, 0, 0, 0, 0, 0] \quad \left(\text{for Ap}^2\text{q etc.}\right) \tag{84}$$

$$[\theta]_{18} = [1, 0, 0, 0; 1, 1, 1, 0, 0, 0, 0, 0] \quad \left(\text{for Ap}\overline{\text{p}}\text{q etc.}\right) \tag{85}$$

$$[\theta]_{19} = [1, 0, 0, 0; 1, 0, 1, 0, 1, 0, 0, 0] \quad \left(\text{for Apqr etc.}\right) \tag{86}$$

In addition, partitions with no achiral proligands are listed as follows:

$$[\theta]_{20} = [0, 0, 0, 0; 4, 0, 0, 0, 0, 0, 0, 0] \quad \left(\text{for p}^4\text{etc.}\right) \tag{87}$$

$$[\theta]_{21} = [0, 0, 0, 0; 3, 1, 0, 0, 0, 0, 0, 0] \quad \left(\text{for p}^3\overline{\text{p}}\text{etc.}\right) \tag{88}$$

$$[\theta]_{22} = [0, 0, 0, 0; 3, 0, 1, 0, 0, 0, 0, 0] \quad \left(\text{for p}^3\text{q etc.}\right) \tag{89}$$

$$[\theta]_{23} = [0, 0, 0, 0; 2, 2, 0, 0, 0, 0, 0, 0] \quad \left(\text{for p}^2\overline{\text{p}}^2\text{etc.}\right) \tag{90}$$

$$[\theta]_{24} = [0, 0, 0, 0; 2, 1, 1, 0, 0, 0, 0, 0] \quad \left(\text{for p}^2\overline{\text{p}}\text{ q etc.}\right) \tag{91}$$

$$[\theta]_{25} = [0, 0, 0, 0; 2, 0, 2, 0, 0, 0, 0, 0] \quad \left(\text{for p}^2\text{q}^2\text{etc.}\right) \tag{92}$$

$$[\theta]_{26} = [0, 0, 0, 0; 2, 0, 1, 1, 0, 0, 0, 0] \quad \left(\text{for p}^2\text{q}\overline{\text{q}}\text{etc.}\right) \tag{93}$$

$$[\theta]_{27} = [0, 0, 0, 0; 2, 0, 1, 0, 1, 0, 0, 0] \quad \left(\text{for p}^2\text{qr etc.}\right) \tag{94}$$

$$[\theta]_{28} = [0, 0, 0, 0; 1, 1, 1, 1, 0, 0, 0, 0] \quad \left(\text{for p }\overline{\text{p}}\text{q}\overline{\text{q}}\text{etc.}\right) \tag{95}$$

$$[\theta]_{29} = [0, 0, 0, 0; 1, 1, 1, 0, 1, 0, 0, 0] \quad \left(\text{for p}\overline{\text{p}}\text{qr etc.}\right) \tag{96}$$

$$[\theta]_{30} = [0, 0, 0, 0; 1, 0, 1, 0, 1, 0, 1, 0] \quad \left(\text{for pqrs etc.}\right) \tag{97}$$

For example, let us examine the SCI-CF (USCI-CF) for $\mathbf{D}_{2d\widetilde{\sigma}\widehat{I}}(/\mathbf{C}_{s\widetilde{\sigma}\widehat{I}}) \downarrow \mathbf{C}_s$, i.e., $a_1^2 c_2$ (cf. the 6th row of Table 3), into which the ligand-inventory functions (Eqs. 64–66) are introduced. The resulting equation is expanded to give the following generating function:

$$\begin{aligned} g_{\mathbf{C}_s} &= \left(\mathrm{A}+\mathrm{B}+\mathrm{X}+\mathrm{Y}\right)^2\left(\mathrm{A}^2+\mathrm{B}^2+\mathrm{X}^2+\mathrm{Y}^2+2\mathrm{p}\overline{\mathrm{p}}+2\mathrm{q}\overline{\mathrm{q}}+2\mathrm{r}\overline{\mathrm{r}}+2\mathrm{s}\overline{\mathrm{s}}\right) \\ &= \left\{\mathrm{A}^4+\mathrm{B}^4+\mathrm{X}^4+\mathrm{Y}^4\right\}+\left\{2\mathrm{A}^3\mathrm{B}+2\mathrm{A}^3\mathrm{X}+2\mathrm{A}^3\mathrm{Y}+\cdots\right\}+ \\ &\quad \left\{2\mathrm{A}^2\mathrm{B}^2+2\mathrm{A}^2\mathrm{X}^2+\cdots\right\}+\left\{2\mathrm{A}^2\mathrm{B}\mathrm{X}+2\mathrm{A}^2\mathrm{B}\mathrm{Y}+\cdots\right\}+ \\ &\quad \left\{2\mathrm{A}^2\mathrm{p}\overline{\mathrm{p}}+2\mathrm{A}^2\mathrm{q}\overline{\mathrm{q}}+\cdots\right\}+\left\{4\mathrm{A}\mathrm{B}\mathrm{p}\overline{\mathrm{p}}+4\mathrm{A}\mathrm{B}\mathrm{q}\overline{\mathrm{q}}+\cdots\right\}, \end{aligned} \tag{98}$$

where the terms of each pair of braces in the last side are represented collectively by a partition selected form $[\theta]_i$ ($i = 1$–30). Let the symbol $\rho_{[\theta]_i\acute{\mathbf{G}}_j}$ be the coefficient of the term corresponding to $[\theta]_i$ ($i = 1$–30) and $\acute{\mathbf{G}}_j$ ($\subset \mathbf{D}_{2d\widetilde{\sigma}\widehat{I}}$). The data calculated by Eq. 98 are represented as follows:

$$\rho_{[\theta]_1\mathbf{C}_s} = 1 \tag{99}$$
$$\rho_{[\theta]_2\mathbf{C}_s} = 2 \tag{100}$$
$$\rho_{[\theta]_4\mathbf{C}_s} = 2 \tag{101}$$
$$\rho_{[\theta]_6\mathbf{C}_s} = 2 \tag{102}$$
$$\rho_{[\theta]_8\mathbf{C}_s} = 2 \tag{103}$$
$$\rho_{[\theta]_{13}\mathbf{C}_s} = 4 \tag{104}$$

This procedure is repeated to cover all the subgroups contained in $\mathrm{SSG}_{\mathbf{D}_{2d\widetilde{\sigma}\widehat{I}}}$ (Eq. 54) by using the data of Table 3. Thereby, we obtain $\rho_{[\theta]_i\acute{\mathbf{G}}_j}$ for $\acute{\mathbf{G}}_j$ ($\in \mathrm{SSG}_{\mathbf{D}_{2d\widetilde{\sigma}\widehat{I}}}$), which are collected so as to give an FPV for symmetry-itemized enumeration for a respective partition $[\theta]_i$ ($i = 1$–30):

$$\begin{aligned} &\mathrm{FPV}_{[\theta]_1} \\ &\quad = \left(\rho_{[\theta]_1\mathbf{C}_1},\ldots,\rho_{[\theta]_1\mathbf{C}_s},\ldots,\rho_{[\theta]_1\acute{\mathbf{G}}_j},\ldots,\rho_{[\theta]_1\mathbf{D}_{2d\widetilde{\sigma}\widehat{I}}}\right) \\ &\quad = (1,1,1,1,1,1,1,1,1,1,1,1,1,1,1,1,1,1,1,1,1,1,1,1,1,1,1). \end{aligned} \tag{105}$$

$$\begin{aligned} &\mathrm{FPV}_{[\theta]_2} \\ &\quad = \left(\rho_{[\theta]_2\mathbf{C}_1},\ldots,\rho_{[\theta]_2\mathbf{C}_s},\ldots,\rho_{[\theta]_2\acute{\mathbf{G}}_j},\ldots,\rho_{[\theta]_2\mathbf{D}_{2d\widetilde{\sigma}\widehat{I}}}\right) \\ &\quad = (4,0,0,2,0,2,4,0,0,0,0,0,0,2,0,0,0,0,0,0,0,0,0,0,0,0,0) \end{aligned} \tag{106}$$

(omitted)

Note that the values $\rho_{[\theta]_1\mathbf{C}_s}$ (Eq. 99) and $\rho_{[\theta]_2\mathbf{C}_s}$ (Eq. 100) appear at the 6th positions of the respective FPVs (Eqs. 105 and 106).

According to Theorem 19.4 (coupled with Theorem 15.4) in [11], the FPVs are multiplied by the inverse $M^{-1}_{\mathbf{D}_{2d\widetilde{\sigma}\widehat{I}}}$ (Eq. 109) to give the following isomer-counting vectors (ICVs):

$$\begin{aligned}\mathrm{ICV}_{[\theta]_1} &= \mathrm{FPV}_{[\theta]_1} \times M^{-1}_{\mathbf{D}_{2d\widetilde{\sigma}\widehat{I}}} \\ &= (0, 0, 0, 0, 0, 0, 0, 0, 0, 0, 0, 0, 0, 0, 0, 0, 0, 0, 0, 0, 0, 0, 0, 0, 0, 0, 1),\end{aligned} \tag{107}$$

$$\begin{aligned}\mathrm{ICV}_{[\theta]_2} &= \mathrm{FPV}_{[\theta]_2} \times M^{-1}_{\mathbf{D}_{2d\widetilde{\sigma}\widehat{I}}} \\ &= (0, 0, 0, 0, 0, 0, 0, 0, 0, 0, 0, 0, 1, 0, 0, 0, 0, 0, 0, 0, 0, 0, 0, 0, 0, 0, 0),\end{aligned} \tag{108}$$

(omitted)

The inverse mark table $M^{-1}_{\mathbf{D}_{2d\widetilde{\sigma}\widehat{I}}}$ is calculated by starting from the mark table $M_{\mathbf{D}_{2d\widetilde{\sigma}\widehat{I}}}$, which is identical with the mark table $M_{\mathbf{D}_{4h}}$ reported previously in [39]. Thus, we obtain:

$$M^{-1}_{\mathbf{D}_{2d\widetilde{\sigma}\widehat{I}}} = M^{-1}_{\mathbf{D}_{4h}} = \left(\overline{m}_{ji}\right)$$

$$= \left(\begin{array}{ccccccccccccccccccccccccccc}
1/16 & 0 & 0 & 0 & 0 & 0 & 0 & 0 & 0 & 0 & 0 & 0 & 0 & 0 & 0 & 0 & 0 & 0 & 0 & 0 & 0 & 0 & 0 & 0 & 0 & 0 & 0 \\
-1/16 & 1/8 & 0 & 0 & 0 & 0 & 0 & 0 & 0 & 0 & 0 & 0 & 0 & 0 & 0 & 0 & 0 & 0 & 0 & 0 & 0 & 0 & 0 & 0 & 0 & 0 & 0 \\
-1/8 & 0 & 1/4 & 0 & 0 & 0 & 0 & 0 & 0 & 0 & 0 & 0 & 0 & 0 & 0 & 0 & 0 & 0 & 0 & 0 & 0 & 0 & 0 & 0 & 0 & 0 & 0 \\
-1/8 & 0 & 0 & 1/4 & 0 & 0 & 0 & 0 & 0 & 0 & 0 & 0 & 0 & 0 & 0 & 0 & 0 & 0 & 0 & 0 & 0 & 0 & 0 & 0 & 0 & 0 & 0 \\
-1/8 & 0 & 0 & 0 & 1/4 & 0 & 0 & 0 & 0 & 0 & 0 & 0 & 0 & 0 & 0 & 0 & 0 & 0 & 0 & 0 & 0 & 0 & 0 & 0 & 0 & 0 & 0 \\
-1/8 & 0 & 0 & 0 & 0 & 1/4 & 0 & 0 & 0 & 0 & 0 & 0 & 0 & 0 & 0 & 0 & 0 & 0 & 0 & 0 & 0 & 0 & 0 & 0 & 0 & 0 & 0 \\
-1/16 & 0 & 0 & 0 & 0 & 0 & 1/8 & 0 & 0 & 0 & 0 & 0 & 0 & 0 & 0 & 0 & 0 & 0 & 0 & 0 & 0 & 0 & 0 & 0 & 0 & 0 & 0 \\
-1/16 & 0 & 0 & 0 & 0 & 0 & 0 & 1/8 & 0 & 0 & 0 & 0 & 0 & 0 & 0 & 0 & 0 & 0 & 0 & 0 & 0 & 0 & 0 & 0 & 0 & 0 & 0 \\
0 & -1/8 & 0 & 0 & 0 & 0 & 0 & 0 & 1/4 & 0 & 0 & 0 & 0 & 0 & 0 & 0 & 0 & 0 & 0 & 0 & 0 & 0 & 0 & 0 & 0 & 0 & 0 \\
0 & -1/8 & 0 & 0 & 0 & 0 & 0 & 0 & 0 & 1/4 & 0 & 0 & 0 & 0 & 0 & 0 & 0 & 0 & 0 & 0 & 0 & 0 & 0 & 0 & 0 & 0 & 0 \\
1/8 & -1/8 & 0 & 0 & -1/4 & 0 & 0 & 0 & 0 & 0 & 1/4 & 0 & 0 & 0 & 0 & 0 & 0 & 0 & 0 & 0 & 0 & 0 & 0 & 0 & 0 & 0 & 0 \\
1/8 & -1/8 & 0 & 0 & 0 & -1/4 & 0 & 0 & 0 & 0 & 0 & 1/4 & 0 & 0 & 0 & 0 & 0 & 0 & 0 & 0 & 0 & 0 & 0 & 0 & 0 & 0 & 0 \\
1/4 & 0 & -1/4 & 0 & -1/4 & 0 & -1/4 & 0 & 0 & 0 & 0 & 0 & 1/2 & 0 & 0 & 0 & 0 & 0 & 0 & 0 & 0 & 0 & 0 & 0 & 0 & 0 & 0 \\
1/4 & 0 & 0 & -1/4 & 0 & -1/4 & -1/4 & 0 & 0 & 0 & 0 & 0 & 0 & 1/2 & 0 & 0 & 0 & 0 & 0 & 0 & 0 & 0 & 0 & 0 & 0 & 0 & 0 \\
1/8 & -1/8 & 0 & 0 & 0 & 0 & -1/8 & -1/8 & 0 & 0 & 0 & 0 & 0 & 0 & 1/4 & 0 & 0 & 0 & 0 & 0 & 0 & 0 & 0 & 0 & 0 & 0 & 0 \\
1/4 & 0 & -1/4 & 0 & -1/4 & 0 & 0 & -1/4 & 0 & 0 & 0 & 0 & 0 & 0 & 0 & 1/2 & 0 & 0 & 0 & 0 & 0 & 0 & 0 & 0 & 0 & 0 & 0 \\
1/4 & 0 & 0 & -1/4 & 0 & -1/4 & 0 & -1/4 & 0 & 0 & 0 & 0 & 0 & 0 & 0 & 0 & 1/2 & 0 & 0 & 0 & 0 & 0 & 0 & 0 & 0 & 0 & 0 \\
1/8 & -1/8 & -1/4 & 0 & 0 & 0 & 0 & 0 & 0 & 0 & 0 & 0 & 0 & 0 & 0 & 0 & 0 & 1/4 & 0 & 0 & 0 & 0 & 0 & 0 & 0 & 0 & 0 \\
1/8 & -1/8 & 0 & -1/4 & 0 & 0 & 0 & 0 & 0 & 0 & 0 & 0 & 0 & 0 & 0 & 0 & 0 & 0 & 1/4 & 0 & 0 & 0 & 0 & 0 & 0 & 0 & 0 \\
0 & 1/4 & 0 & 0 & 0 & 0 & 0 & 0 & -1/4 & 0 & -1/4 & -1/4 & 0 & 0 & 0 & 0 & 0 & 0 & 0 & 1/2 & 0 & 0 & 0 & 0 & 0 & 0 & 0 \\
0 & 1/4 & 0 & 0 & 0 & 0 & 0 & 0 & -1/4 & -1/4 & 0 & 0 & 0 & 0 & -1/4 & 0 & 0 & 0 & 0 & 0 & 1/2 & 0 & 0 & 0 & 0 & 0 & 0 \\
0 & 1/4 & 0 & 0 & 0 & 0 & 0 & 0 & 0 & -1/4 & 0 & -1/4 & 0 & 0 & 0 & 0 & 0 & -1/4 & 0 & 0 & 0 & 1/2 & 0 & 0 & 0 & 0 & 0 \\
0 & 1/4 & 0 & 0 & 0 & 0 & 0 & 0 & 0 & -1/4 & -1/4 & 0 & 0 & 0 & 0 & 0 & 0 & 0 & -1/4 & 0 & 0 & 0 & 1/2 & 0 & 0 & 0 & 0 \\
-1/2 & 1/4 & 1/2 & 0 & 1/2 & 0 & 1/4 & 1/4 & 0 & 0 & -1/4 & 0 & -1/2 & 0 & -1/4 & -1/2 & 0 & -1/4 & 0 & 0 & 0 & 0 & 0 & 1/2 & 0 & 0 & 0 \\
-1/2 & 1/4 & 0 & 1/2 & 0 & 1/2 & 1/4 & 1/4 & 0 & 0 & 0 & -1/4 & 0 & -1/2 & -1/4 & 0 & -1/2 & 0 & -1/4 & 0 & 0 & 0 & 0 & 0 & 1/2 & 0 & 0 \\
0 & 1/4 & 0 & 0 & 0 & 0 & 0 & 0 & -1/4 & 0 & 0 & 0 & 0 & 0 & 0 & 0 & 0 & -1/4 & -1/4 & 0 & 0 & 0 & 0 & 0 & 0 & 1/2 & 0 \\
0 & -1 & 0 & 0 & 0 & 0 & 0 & 0 & 1/2 & 1/2 & 1/2 & 1/2 & 0 & 0 & 1/2 & 0 & 0 & 1/2 & 1/2 & -1/2 & -1/2 & -1/2 & -1/2 & -1/2 & -1/2 & -1/2 & 1
\end{array}\right) \tag{109}$$

By referring to $\mathrm{SSG}_{\mathbf{D}_{2d\widetilde{\sigma}\widehat{I}}}$ (Eq. 54), Eq. 107 indicates that one promolecule (a quadruplet) as an *RS*-stereoisomer with $[\theta]_1$ (A^4 etc.) exists to belong to $\mathbf{D}_{2d\widetilde{\sigma}\widehat{I}}$, while Eq. 108 indicates that one promolecule (a quadruplet) as an *RS*-stereoisomer with $[\theta]_2$ (A^3B etc.) exists to belong to $\mathbf{C}_{s\widetilde{\sigma}\widehat{I}}$.

5.2 Fixed-point matrices for symmetry-itemized enumeration

For the purpose of systematic enumeration of allenes, several FPVs can be collected as row vectors of a matrix, which is called *a fixed-point matrix* (FPM) according to Sections 15.2 and 19.2 of [11]. By collecting the FPVs for the partitions $[\theta]_1$–$[\theta]_{19}$ (cf. Eqs. 105 and 106 for obtaining $\mathrm{FPV}_{[\theta]_1}$ and $\mathrm{FPV}_{[\theta]_2}$), we obtain the following FPM:

$$
\mathrm{FPM}_1 = \begin{array}{c} [\theta]_1 \\ [\theta]_2 \\ [\theta]_3 \\ [\theta]_4 \\ [\theta]_5 \\ [\theta]_6 \\ [\theta]_7 \\ [\theta]_8 \\ [\theta]_9 \\ [\theta]_{10} \\ [\theta]_{11} \\ [\theta]_{12} \\ [\theta]_{13} \\ [\theta]_{14} \\ [\theta]_{15} \\ [\theta]_{16} \\ [\theta]_{17} \\ [\theta]_{18} \\ [\theta]_{19} \end{array}
\left[\begin{array}{ccccccccccccccccccccccccccc}
1&1&1&1&1&1&1&1&1&1&1&1&1&1&1&1&1&1&1&1&1&1&1&1&1&1&1 \\
4&0&0&2&0&2&4&0&0&0&0&0&0&2&0&0&0&0&0&0&0&0&0&0&0&0&0 \\
4&0&0&2&0&0&0&0&0&0&0&0&0&0&0&0&0&0&0&0&0&0&0&0&0&0&0 \\
6&2&2&2&2&2&6&2&0&0&0&2&2&2&2&0&2&0&2&0&0&0&0&0&2&0&0 \\
6&2&2&2&0&0&0&0&0&0&0&0&0&0&0&0&0&0&2&0&0&0&0&0&0&0&0 \\
12&0&0&2&0&2&12&0&0&0&0&0&0&2&0&0&0&0&0&0&0&0&0&0&0&0&0 \\
12&0&0&2&0&0&0&0&0&0&0&0&0&0&0&0&0&0&0&0&0&0&0&0&0&0&0 \\
12&0&0&2&4&2&0&4&0&0&0&0&0&0&0&0&2&0&0&0&0&0&0&0&0&0&0 \\
12&0&0&2&0&0&0&0&0&0&0&0&0&0&0&0&0&0&0&0&0&0&0&0&0&0&0 \\
24&0&0&0&0&0&24&0&0&0&0&0&0&0&0&0&0&0&0&0&0&0&0&0&0&0&0 \\
24&0&0&0&0&0&0&0&0&0&0&0&0&0&0&0&0&0&0&0&0&0&0&0&0&0&0 \\
12&0&0&2&0&0&0&0&0&0&0&0&0&0&0&0&0&0&0&0&0&0&0&0&0&0&0 \\
24&0&0&0&0&4&0&0&0&0&0&0&0&0&0&0&0&0&0&0&0&0&0&0&0&0&0 \\
24&0&0&0&0&0&0&0&0&0&0&0&0&0&0&0&0&0&0&0&0&0&0&0&0&0&0 \\
4&0&0&2&0&0&0&0&0&0&0&0&0&0&0&0&0&0&0&0&0&0&0&0&0&0&0 \\
12&0&0&2&0&0&0&0&0&0&0&0&0&0&0&0&0&0&0&0&0&0&0&0&0&0&0 \\
12&0&0&2&0&0&0&0&0&0&0&0&0&0&0&0&0&0&0&0&0&0&0&0&0&0&0 \\
24&0&0&0&0&0&0&0&0&0&0&0&0&0&0&0&0&0&0&0&0&0&0&0&0&0&0 \\
24&0&0&0&0&0&0&0&0&0&0&0&0&0&0&0&0&0&0&0&0&0&0&0&0&0&0
\end{array}\right] \tag{110}
$$

where the values collected in each column appear as the coefficients of the terms which correspond to the partitions $[\theta]_i$ ($i = 1$ to 19), appearing in the generating function of the *RS*-stereoisomeric group of the column. Thus, the coefficients of respective terms in the generating function $g_{\mathbf{C}_s}$ (Eq. 98) appear in the $\mathbf{C}_s$-column (the 6th column) of the FPM_1 (Eq. 110), where non-zero values appear in the $[\theta]_1$-row (for A^4 etc.), the $[\theta]_2$-row (for $\mathrm{A}^3\mathrm{B}$ etc.), the $[\theta]_4$-row (for $\mathrm{A}^2\mathrm{B}^2$ etc.), the $[\theta]_6$-row (for $\mathrm{A}^2\mathrm{BX}$ etc.), the $[\theta]_8$-row (for $\mathrm{A}^2\mathrm{p}\overline{\mathrm{p}}$etc.), and the $[\theta]_{13}$-row (for $\mathrm{ABp}\overline{\mathrm{p}}$ etc.).

Because the FPM (Eq. 110) contains FPVs as its row vectors, it is multiplied by the inverse $M^{-1}_{\mathbf{D}_{2d\widetilde{\sigma}\widehat{I}}}$ (Eq. 109), so as to give an isomer-counting matrix (ICM_1):

$$
\mathrm{ICM}_1 = \mathrm{FPM}_1 \times M^{-1}_{\mathbf{D}_{2d\widetilde{\sigma}\widehat{I}}}
$$

$$
= \begin{array}{c} [\theta]_1 \\ [\theta]_2 \\ [\theta]_3 \\ [\theta]_4 \\ [\theta]_5 \\ [\theta]_6 \\ [\theta]_7 \\ [\theta]_8 \\ [\theta]_9 \\ [\theta]_{10} \\ [\theta]_{11} \\ [\theta]_{12} \\ [\theta]_{13} \\ [\theta]_{14} \\ [\theta]_{15} \\ [\theta]_{16} \\ [\theta]_{17} \\ [\theta]_{18} \\ [\theta]_{19} \end{array}
\left[\begin{array}{cccccccccc|cccccccccc|ccccccc}
0&0&0&0&0&0&0&0&0&0&0&0&0&0&0&0&0&0&0&0&0&0&0&0&0&0&1 \\
0&0&0&0&0&0&0&0&0&0&0&0&0&1&0&0&0&0&0&0&0&0&0&0&0&0&0 \\
0&0&0&1/2&0&0&0&0&0&0&0&0&0&0&0&0&0&0&0&0&0&0&0&0&0&0&0 \\
0&0&0&0&0&0&0&0&0&0&0&0&1&0&0&0&0&0&0&0&0&0&0&0&1&0&0 \\
0&0&1/2&0&0&0&0&0&0&0&0&0&0&0&0&0&0&0&1/2&0&0&0&0&0&0&0&0 \\
0&0&0&0&0&0&1&0&0&0&0&0&0&1&0&0&0&0&0&0&0&0&0&0&0&0&0 \\
1/2&0&0&1/2&0&0&0&0&0&0&0&0&0&0&0&0&0&0&0&0&0&0&0&0&0&0&0 \\
0&0&0&0&1&0&0&0&0&0&0&0&0&0&0&0&1&0&0&0&0&0&0&0&0&0&0 \\
1/2&0&0&1/2&0&0&0&0&0&0&0&0&0&0&0&0&0&0&0&0&0&0&0&0&0&0&0 \\
0&0&0&0&0&0&3&0&0&0&0&0&0&0&0&0&0&0&0&0&0&0&0&0&0&0&0 \\
3/2&0&0&0&0&0&0&0&0&0&0&0&0&0&0&0&0&0&0&0&0&0&0&0&0&0&0 \\
1/2&0&0&1/2&0&0&0&0&0&0&0&0&0&0&0&0&0&0&0&0&0&0&0&0&0&0&0 \\
1&0&0&0&0&1&0&0&0&0&0&0&0&0&0&0&0&0&0&0&0&0&0&0&0&0&0 \\
3/2&0&0&0&0&0&0&0&0&0&0&0&0&0&0&0&0&0&0&0&0&0&0&0&0&0&0 \\
0&0&0&1/2&0&0&0&0&0&0&0&0&0&0&0&0&0&0&0&0&0&0&0&0&0&0&0 \\
1/2&0&0&1/2&0&0&0&0&0&0&0&0&0&0&0&0&0&0&0&0&0&0&0&0&0&0&0 \\
1/2&0&0&1/2&0&0&0&0&0&0&0&0&0&0&0&0&0&0&0&0&0&0&0&0&0&0&0 \\
3/2&0&0&0&0&0&0&0&0&0&0&0&0&0&0&0&0&0&0&0&0&0&0&0&0&0&0 \\
3/2&0&0&0&0&0&0&0&0&0&0&0&0&0&0&0&0&0&0&0&0&0&0&0&0&0&0
\end{array}\right] \tag{111}
$$

where vertical lines are added at every ten columns for the sake of convenience. The j-th column corresponds to the subgroup $\acute{\mathbf{G}}_j$ collected in Table 3. The ICM_1 contains the resulting ICVs as its row vectors, so that the $[\theta]_1$- and the $[\theta]_2$-rows are identical with the vectors shown in Eqs. 107 and 108.

The value $\frac{1}{2}$ at the intersection between the $[\theta]_3$-row and $\mathbf{C}_{\widetilde{\sigma}}$-column (the 4th column) in the ICM_1 (Eq. 111) corresponds to the term $\frac{1}{2}(\mathrm{A}^3\mathrm{p} + \mathrm{A}^3\overline{\mathrm{p}})$, which indicates that an enantiomeric pair is counted once as a quadruplet.

The FPM can be constructed from the data of generating functions (e.g., Eq. 98) by applying the procedure described above:

$$\mathrm{FPM}_2 = \begin{array}{c} [\theta]_{20} \\ [\theta]_{21} \\ [\theta]_{22} \\ [\theta]_{23} \\ [\theta]_{24} \\ [\theta]_{25} \\ [\theta]_{26} \\ [\theta]_{27} \\ [\theta]_{28} \\ [\theta]_{29} \\ [\theta]_{30} \end{array} \left[\begin{array}{ccccccccccccccccccccccccccc}
1 & 1 & 1 & 1 & 0 & 0 & 0 & 0 & 1 & 0 & 0 & 0 & 0 & 0 & 0 & 0 & 1 & 1 & 0 & 0 & 0 & 0 & 0 & 0 & 0 & 1 & 0 \\
4 & 0 & 0 & 2 & 0 & 0 & 0 & 0 & 0 & 0 & 0 & 0 & 0 & 0 & 0 & 0 & 0 & 0 & 0 & 0 & 0 & 0 & 0 & 0 & 0 & 0 & 0 \\
4 & 0 & 0 & 2 & 0 & 0 & 0 & 0 & 0 & 0 & 0 & 0 & 0 & 0 & 0 & 0 & 0 & 0 & 0 & 0 & 0 & 0 & 0 & 0 & 0 & 0 & 0 \\
6 & 2 & 2 & 2 & 4 & 0 & 0 & 4 & 0 & 2 & 2 & 0 & 0 & 0 & 0 & 2 & 0 & 0 & 2 & 0 & 0 & 0 & 2 & 0 & 0 & 0 & 0 \\
12 & 0 & 0 & 2 & 0 & 0 & 0 & 0 & 0 & 0 & 0 & 0 & 0 & 0 & 0 & 0 & 0 & 0 & 0 & 0 & 0 & 0 & 0 & 0 & 0 & 0 & 0 \\
6 & 2 & 2 & 2 & 0 & 0 & 0 & 0 & 0 & 0 & 0 & 0 & 0 & 0 & 0 & 0 & 0 & 0 & 2 & 0 & 0 & 0 & 0 & 0 & 0 & 0 & 0 \\
12 & 0 & 0 & 2 & 0 & 0 & 0 & 0 & 0 & 0 & 0 & 0 & 0 & 0 & 0 & 0 & 0 & 0 & 0 & 0 & 0 & 0 & 0 & 0 & 0 & 0 & 0 \\
12 & 0 & 0 & 2 & 0 & 0 & 0 & 0 & 0 & 0 & 0 & 0 & 0 & 0 & 0 & 0 & 0 & 0 & 0 & 0 & 0 & 0 & 0 & 0 & 0 & 0 & 0 \\
24 & 0 & 0 & 0 & 8 & 0 & 0 & 8 & 0 & 0 & 0 & 0 & 0 & 0 & 0 & 0 & 0 & 0 & 0 & 0 & 0 & 0 & 0 & 0 & 0 & 0 & 0 \\
24 & 0 & 0 & 0 & 0 & 0 & 0 & 0 & 0 & 0 & 0 & 0 & 0 & 0 & 0 & 0 & 0 & 0 & 0 & 0 & 0 & 0 & 0 & 0 & 0 & 0 & 0 \\
24 & 0 & 0 & 0 & 0 & 0 & 0 & 0 & 0 & 0 & 0 & 0 & 0 & 0 & 0 & 0 & 0 & 0 & 0 & 0 & 0 & 0 & 0 & 0 & 0 & 0 & 0
\end{array}\right] \tag{112}$$

The FPM (Eq. 112) is multiplied by $M^{-1}_{\mathbf{D}_{2d\widetilde{\sigma}\widehat{I}}}$ (Eq. 109), so as to give another isomer-counting matrix (ICM_2):

$$\begin{aligned} \mathrm{ICM}_2 &= \mathrm{FPM}_2 \times M^{-1}_{\mathbf{D}_{2d\widetilde{\sigma}\widehat{I}}} \\ &= \begin{array}{c} [\theta]_{20} \\ [\theta]_{21} \\ [\theta]_{22} \\ [\theta]_{23} \\ [\theta]_{24} \\ [\theta]_{25} \\ [\theta]_{26} \\ [\theta]_{27} \\ [\theta]_{28} \\ [\theta]_{29} \\ [\theta]_{30} \end{array} \left[\begin{array}{cccccccccc|cccccccccc|ccccccc}
0 & 0 & 0 & 0 & 0 & 0 & 0 & 0 & 0 & 0 & 0 & 0 & 0 & 0 & 0 & 0 & 0 & 0 & 0 & 0 & 0 & 0 & 0 & 0 & 0 & 1/2 & 0 \\
0 & 0 & 0 & 1/2 & 0 & 0 & 0 & 0 & 0 & 0 & 0 & 0 & 0 & 0 & 0 & 0 & 0 & 0 & 0 & 0 & 0 & 0 & 0 & 0 & 0 & 0 & 0 \\
0 & 0 & 0 & 1/2 & 0 & 0 & 0 & 0 & 0 & 0 & 0 & 0 & 0 & 0 & 0 & 0 & 0 & 0 & 0 & 0 & 0 & 0 & 0 & 0 & 0 & 0 & 0 \\
0 & 0 & 0 & 0 & 0 & 0 & 0 & 0 & 0 & 0 & 0 & 0 & 0 & 0 & 0 & 1 & 0 & 0 & 0 & 0 & 0 & 0 & 1 & 0 & 0 & 0 & 0 \\
1/2 & 0 & 0 & 1/2 & 0 & 0 & 0 & 0 & 0 & 0 & 0 & 0 & 0 & 0 & 0 & 0 & 0 & 0 & 0 & 0 & 0 & 0 & 0 & 0 & 0 & 0 & 0 \\
0 & 0 & 1/2 & 0 & 0 & 0 & 0 & 0 & 0 & 0 & 0 & 0 & 0 & 0 & 0 & 0 & 0 & 0 & 1/2 & 0 & 0 & 0 & 0 & 0 & 0 & 0 & 0 \\
1/2 & 0 & 0 & 1/2 & 0 & 0 & 0 & 0 & 0 & 0 & 0 & 0 & 0 & 0 & 0 & 0 & 0 & 0 & 0 & 0 & 0 & 0 & 0 & 0 & 0 & 0 & 0 \\
1/2 & 0 & 0 & 1/2 & 0 & 0 & 0 & 0 & 0 & 0 & 0 & 0 & 0 & 0 & 0 & 0 & 0 & 0 & 0 & 0 & 0 & 0 & 0 & 0 & 0 & 0 & 0 \\
0 & 0 & 0 & 0 & 2 & 0 & 0 & 1 & 0 & 0 & 0 & 0 & 0 & 0 & 0 & 0 & 0 & 0 & 0 & 0 & 0 & 0 & 0 & 0 & 0 & 0 & 0 \\
3/2 & 0 & 0 & 0 & 0 & 0 & 0 & 0 & 0 & 0 & 0 & 0 & 0 & 0 & 0 & 0 & 0 & 0 & 0 & 0 & 0 & 0 & 0 & 0 & 0 & 0 & 0 \\
3/2 & 0 & 0 & 0 & 0 & 0 & 0 & 0 & 0 & 0 & 0 & 0 & 0 & 0 & 0 & 0 & 0 & 0 & 0 & 0 & 0 & 0 & 0 & 0 & 0 & 0 & 0
\end{array}\right] \end{aligned} \tag{113}$$

where vertical lines are added at every ten columns for the sake of convenience. The j-th column corresponds to the subgroup $\acute{\mathbf{G}}_j$ collected in Table 3.

5.3 Quadruplets for characterizing allene derivatives

5.3.1 Stereoisograms of five types itemized by RS-stereoisomeric groups

As shown in Fig. 4, the 27 subgroups of the *RS*-stereoisomeric group $\mathbf{D}_{2d\widetilde{\sigma}\widehat{I}}$ are categorized into five types:

$$\text{Type I: } \mathrm{SG}^{[\mathrm{I}]} = \{\overset{5}{\mathbf{C}_{\widehat{\sigma}}}, \overset{7}{\mathbf{C}_{\widehat{I}}}, \overset{8}{\mathbf{C}_{\widehat{\sigma}'}}, \overset{11}{\mathbf{C}_{2\widehat{\sigma}}}, \overset{13}{\mathbf{C}_{2\widehat{I}}}, \overset{15}{\mathbf{C}'_{2\widehat{I}}}, \overset{16}{\mathbf{C}'_{2\widehat{\sigma}}}, \overset{24}{\mathbf{D}_{2\widehat{I}}}\} \tag{114}$$

$$\text{Type II: } \mathrm{SG}^{[\mathrm{II}]} = \{\overset{4}{\mathbf{C}_{\widetilde{\sigma}}}, \overset{9}{\mathbf{S}_{\widetilde{4}}}, \overset{19}{\mathbf{C}_{2\widetilde{\sigma}}}, \overset{26}{\mathbf{D}_{2\widetilde{\sigma}}}\} \tag{115}$$

$$\text{Type III: } \mathrm{SG}^{[\mathrm{III}]} = \{\overset{1}{\mathbf{C}_1}, \overset{2}{\mathbf{C}_2}, \overset{3}{\mathbf{C}'_2}, \overset{18}{\mathbf{D}_2}\} \tag{116}$$

$$\text{Type IV: } \mathrm{SG}^{[\mathrm{IV}]} = \{\overset{14}{\mathbf{C}_{s\widetilde{\sigma}\widehat{I}}}, \overset{17}{\mathbf{C}_{s\widetilde{\sigma}\widehat{\sigma}}}, \overset{20}{\mathbf{S}_{\widetilde{4}\widehat{\sigma}}}, \overset{21}{\mathbf{S}_{\widetilde{4}\widehat{I}}}, \overset{23}{\mathbf{S}_{4\widetilde{\sigma}\widehat{\sigma}}}, \overset{25}{\mathbf{C}_{2v\widetilde{\sigma}\widehat{I}}}, \overset{27}{\mathbf{D}_{2d\widetilde{\sigma}\widehat{I}}}\} \tag{117}$$

$$\text{Type V: } \mathrm{SG}^{[\mathrm{V}]} = \{\overset{6}{\mathbf{C}_s}, \overset{10}{\mathbf{S}_4}, \overset{12}{\mathbf{C}_{2v}}, \overset{22}{\mathbf{D}_{2d}}\} \tag{118}$$

Let the symbol **A** denote a representative (a reference promolecule) for specifying each enumerated quadruplet. According to the five categories shown in Eqs. 114–118, there appear stereoisograms of five types, as shown in Fig. 5. This figure is a modification of Fig. 6 of [27] and of Fig. 2 of [40], where the subgroups of $\mathbf{D}_{2d\widetilde{\sigma}\widehat{I}}$ are shown along with three attributes characterizing respective types.

In each stereoisogram of Fig. 5, a reference promolecule located at its upper-left position is represented by using the symbols **A**, which is a representative of a quadruplet contained in the stereoisogram. The vertical equality symbol indicates the achirality of **A**, as found in the type-IV or type-V stereoisogram. The horizontal equality symbol indicates the *RS*-astereogenicity of **A**, as found in the type-II or type-IV stereoisogram. The diagonal equality symbol indicates the asclerality of **A**, as found in the type-I stereoisogram.

The type-I (or type-II) stereoisogram shown in Fig. 5 contains one pair of enantiomers $\mathbf{A}/\overline{\mathbf{A}}$. The type-III stereoisogram shown in Fig. 5 contains two pairs of enantiomers $\mathbf{A}/\overline{\mathbf{A}}$ and $\mathbf{B}/\overline{\mathbf{B}}$. The type-IV stereoisogram shown in Fig. 5 contains one achiral promolecule **A**. The type-V stereoisogram shown in Fig. 5 exhibits pseudoasymmetry, where it contains two achiral promolecules **A** and **B**, which are *RS*-diastereomeric to each other.

5.3.2 List of stereoisograms of allene derivatives itemized by RS-stereoisomeric groups

The isomer-counting matrices (ICMs) shown in Eqs. 111 and 113 contain an itemized value at each intersection between the partition row ($[\theta]_i$; $i = 1$–30) and the subgroup column ($\acute{\mathbf{G}}_j \in \mathrm{SSG}_{\mathbf{D}_{2d\widetilde{\sigma}\widehat{I}}}$, cf. Eq. 54).

Quadruplets of Type I Among the subgroups collected in Eq. 114 (cf. Eqs. 39–46) for characterizing quadruplets of type-I stereoisograms, the itemized enumerations shown in Eqs. 111 and 113 indicate that there appear quadruplets belonging to $\mathbf{C}_{\widehat{\sigma}}$ (the 5th column), $\mathbf{C}_{\widehat{I}}$ (the 7th column), $\mathbf{C}'_{\widehat{\sigma}}$ (the 8th column), $\mathbf{C}_{2\widehat{I}}$ (the 13th column), and $\mathbf{C}'_{2\widehat{\sigma}}$ (the 16th column). A reference promolecule for each enumerated quadruplet is depicted in Fig. 6.

For example, the promolecule **8** with $\mathrm{A}^2\mathrm{B}^2$ corresponds to the partition $[\theta]_4$, so that it belongs to the *RS*-stereoisomeric group $\mathbf{C}_{2\widehat{I}}$, as found in the intersection between the $[\theta]_4$-row and the $\mathbf{C}_{2\widehat{I}}$-column (the 13th column) of Eq. 111. The corresponding

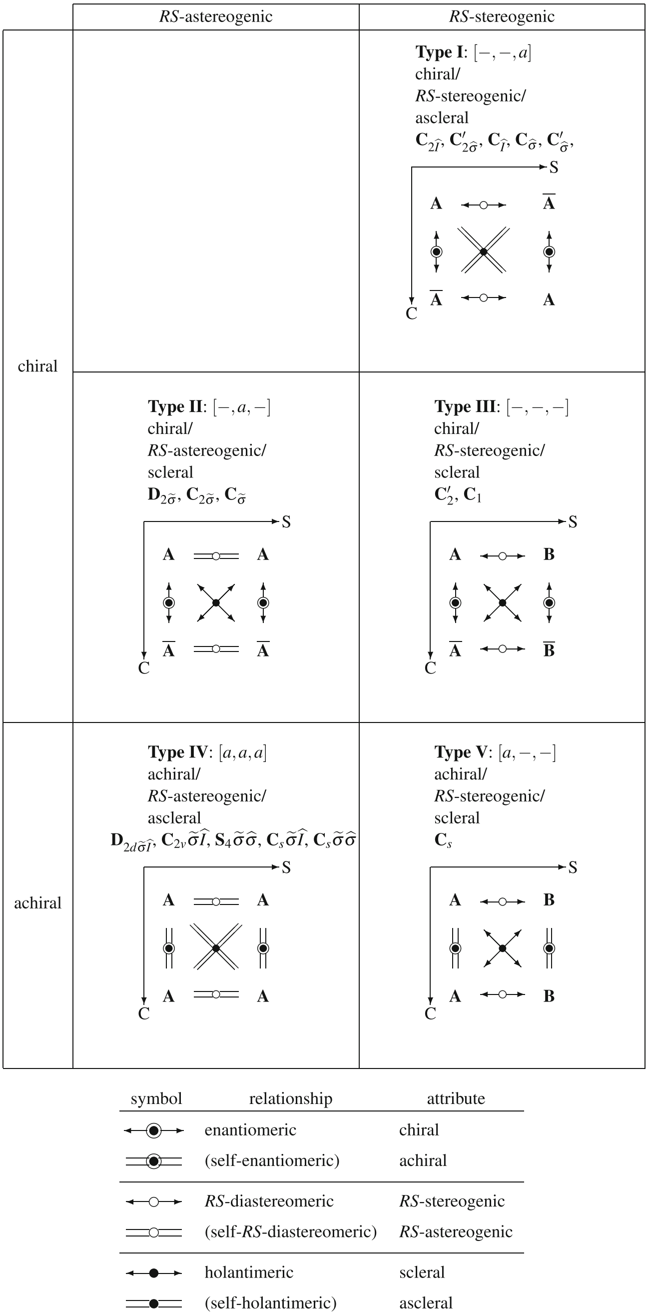

Fig. 5 Stereoisograms for representing RS-stereoisomers of five types, where RS-stereoisomeric subgroups plausible for allene derivatives are listed under the action of $\mathbf{D}_{2d\widetilde{\sigma}\widehat{I}}$. This figure is a modification of Fig. 6 of [27] and of Fig. 2 of [40], where three attributes characterizing respective types are shown along with the subgroups of $\mathbf{D}_{2d\widetilde{\sigma}\widehat{I}}$. The symbols $\mathbf{A}$ and $\overline{\mathbf{A}}$ (or $\mathbf{B}$ and $\overline{\mathbf{B}}$) represent a pair of enantiomers based on an allene skeleton

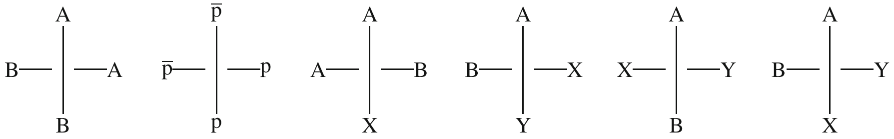

8¶1 ($[\theta]_4$) $\mathbf{C}_{2\widehat{I}}, \mathbf{C}'_2, \mathrm{I}$ | **9**¶2 ($[\theta]_{23}$) $\mathbf{C}'_{2\widehat{\sigma}}, \mathbf{C}'_2, \mathrm{I}$ | **10**¶3 ($[\theta]_6$) $\mathbf{C}_{\widehat{I}}, \mathbf{C}_1, \mathrm{I}$ | **11** ($[\theta]_{10}$) $\mathbf{C}_{\widehat{I}}, \mathbf{C}_1, \mathrm{I}$ | **12** ($[\theta]_{10}$) $\mathbf{C}_{\widehat{I}}, \mathbf{C}_1, \mathrm{I}$ | **13** ($[\theta]_{10}$) $\mathbf{C}_{\widehat{I}}, \mathbf{C}_1, \mathrm{I}$

(11, 12, 13: *)

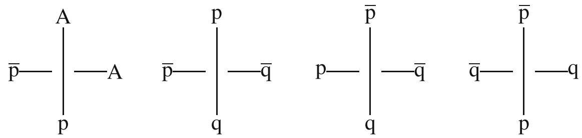

14¶4 ($[\theta]_8$) $\mathbf{C}_{\widehat{\sigma}}, \mathbf{C}_1, \mathrm{I}$ | **15** ($[\theta]_{28}$) $\mathbf{C}_{\widehat{\sigma}}, \mathbf{C}_1, \mathrm{I}$ | **16** ($[\theta]_{28}$) $\mathbf{C}_{\widehat{\sigma}}, \mathbf{C}_1, \mathrm{I}$ | **17** ($[\theta]_{28}$) $\mathbf{C}'_{\widehat{\sigma}}, \mathbf{C}_1, \mathrm{I}$

(15, 16, 17: *)

Fig. 6 Representatives of type-I quadruplets for allene derivatives. The partitions $[\theta]_i$ (i = 1–30) are shown in Eqs. 68–97. The *RS*-stereoisomeric groups of type I are selected from Eqs. 39–46 in accord with enumeration data listed in ICM_1 (Eq. 111) and ICM_2 (Eq. 113). The *RS*-stereoisomeric groups are accompanies with the corresponding point groups and stereoisogram types

stereoisogram of type I is shown in Fig. 5, where an enantiomeric pair of $\mathbf{A}$ and $\overline{\mathbf{A}}$ corresponds to a common term A^2B^2. The subduction at the 13th row of Table 3 indicates the presence of two $\mathbf{C}_{2\widehat{I}}(/\mathbf{C}_{\widehat{I}})$-orbits, which correspond to A^2 and B^2, respectively.

Note that two or more promolecules with the symbol ¶1 (or ¶2 . . . ¶4) have the same partition but belong to different types of *RS*-stereoisomeric groups. For example, **8** with ¶1 (type I in Fig. 6) corresponds to **63** with ¶1 (type IV in Fig. 9), where their enumerated values appear in the $[\theta]_4$-row of Eq. 111. Such promolecules with the same partition are called *isoskeletal isomers* [38], when they are not stereoisomeric.

Three promolecules linked with an underbrace (*) have the same partition but belong to different *RS*-stereoisomeric groups, although they are categorized into the same type (type I). For example, a set of **11,12**, and **13** exhibits isoskeletal isomerism within the type-I category, where its value 3 appears in the $[\theta]_{10}$-row of Eq. 111. Another isoskeletal set of **15,16**, and **17** corresponds to the value 2 (the $\mathbf{C}_{\widehat{\sigma}}$-column or the 5th column for **15** and **16**) and the value 1 (the $\mathbf{C}'_{\widehat{\sigma}}$-column or the 8th column for **17**) in the $[\theta]_{28}$-row of Eq. 113.

Quadruplets of Type II Among the subgroups listed in Eq. 115 (cf. Eqs. 35–38) for characterizing quadruplets of type-II stereoisograms, the itemized enumerations shown in Eqs. 111 and 113 indicate that there appear quadruplets belonging to $\mathbf{C}_{\widetilde{\sigma}}$ (the 4th column), $\mathbf{C}_{2\widetilde{\sigma}}$ (the 19th column), and $\mathbf{D}_{2\widetilde{\sigma}}$ (the 26th column). A reference promolecule for each enumerated quadruplet is depicted in Fig. 7.

For example, the promolecule **19** with A^2p^2 corresponds to the partition $[\theta]_5$, so that it belongs to the *RS*-stereoisomeric group $\mathbf{C}_{2\widetilde{\sigma}}$. The value 1/2 at the

Fig. 7 Representatives of type-II quadruplets for allene derivatives. The partitions $[\theta]_i$ (i = 1–30) are shown in Eqs. 68–97. The *RS*-stereoisomeric groups of type II are selected from Eqs. 35–38 in accord with enumeration data listed in ICM_1 (Eq. 111) and ICM_2 (Eq. 113). The *RS*-stereoisomeric groups are accompanies with the corresponding point groups and stereoisogram types

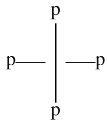

18 ($[\theta]_{20}$)
$\mathbf{D}_{2\widetilde{\sigma}}$, $\mathbf{D}_2$, II

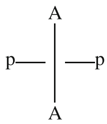

19$^{\dagger 1}$ ($[\theta]_5$)
$\mathbf{C}_{2\widetilde{\sigma}}$, $\mathbf{C}_2$, II

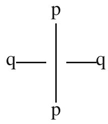

20$^{\dagger 2}$ ($[\theta]_{25}$)
$\mathbf{C}_{2\widetilde{\sigma}}$, $\mathbf{C}_2$, II

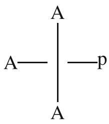

21 ($[\theta]_3$)
$\mathbf{C}_{\widetilde{\sigma}}$, $\mathbf{C}_1$, II

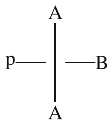

22$^{\dagger 3}$ ($[\theta]_7$)
$\mathbf{C}_{\widetilde{\sigma}}$, $\mathbf{C}_1$, II

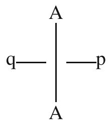

23$^{\dagger 4}$ ($[\theta]_9$)
$\mathbf{C}_{\widetilde{\sigma}}$, $\mathbf{C}_1$, II

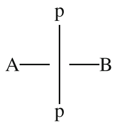

24$^{\dagger 5}$ ($[\theta]_{12}$)
$\mathbf{C}_{\widetilde{\sigma}}$, $\mathbf{C}_1$, II

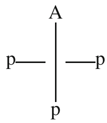

25 ($[\theta]_{15}$)
$\mathbf{C}_{\widetilde{\sigma}}$, $\mathbf{C}_1$, II

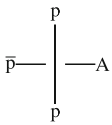

26$^{\dagger 6}$ ($[\theta]_{16}$)
$\mathbf{C}_{\widetilde{\sigma}}$, $\mathbf{C}_1$, II

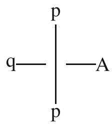

27$^{\dagger 7}$ ($[\theta]_{17}$)
$\mathbf{C}_{\widetilde{\sigma}}$, $\mathbf{C}_1$, II

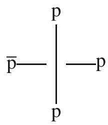

28 ($[\theta]_{21}$)
$\mathbf{C}_{\widetilde{\sigma}}$, $\mathbf{C}_1$, II

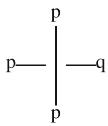

29 ($[\theta]_{22}$)
$\mathbf{C}_{\widetilde{\sigma}}$, $\mathbf{C}_1$, II

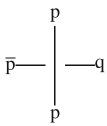

30$^{\dagger 8}$ ($[\theta]_{24}$)
$\mathbf{C}_{\widetilde{\sigma}}$, $\mathbf{C}_1$, II

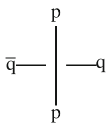

31$^{\dagger 9}$ ($[\theta]_{26}$)
$\mathbf{C}_{\widetilde{\sigma}}$, $\mathbf{C}_1$, II

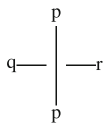

32$^{\dagger 10}$ ($[\theta]_{27}$)
$\mathbf{C}_{\widetilde{\sigma}}$, $\mathbf{C}_1$, II

intersection between the $[\theta]_5$-row and the $\mathbf{C}_{2\widetilde{\sigma}}$-column (the 19th column) of Eq. 111 shows the presence of one quadruplet of $\frac{1}{2}(\mathrm{A}^2\mathrm{p}^2 + \mathrm{A}^2\overline{\mathrm{p}}^2)$. The corresponding stereoisogram of type II is shown in Fig. 5, where $\mathbf{A}$ and $\overline{\mathbf{A}}$ correspond to $\mathrm{A}^2\mathrm{p}^2$ and $\mathrm{A}^2\overline{\mathrm{p}}^2$, respectively. The subduction at the 19th row of Table 3 indicates the presence of one $\mathbf{C}_{2\widetilde{\sigma}}(/\mathbf{C}_{\widetilde{\sigma}})$-orbit ($\mathrm{A}^2$) and one $\mathbf{C}_{2\widetilde{\sigma}}(/\mathbf{C}'_{\widetilde{\sigma}})$-orbit ($\mathrm{p}^2$ or $\overline{\mathrm{p}}^2$).

Two or more promolecules with the symbol †1 (or †2 ⋯ †10) have the same partition but belong to different types of *RS*-stereoisomeric groups. For example, the promolecule **19** with †1 (type II in Fig. 7) corresponds to **33** with †1 (type V in Fig. 8), where their enumerated values appear in the $[\theta]_5$-row of Eq. 111.

Quadruplets of Type III Among the subgroups listed in Eq. 116 (cf. Eqs. 27–30) for characterizing quadruplets of type-III stereoisograms, the itemized enumerations shown in Eqs. 111 and 113 indicate that there appear quadruplets belonging to $\mathbf{C}_1$ (the

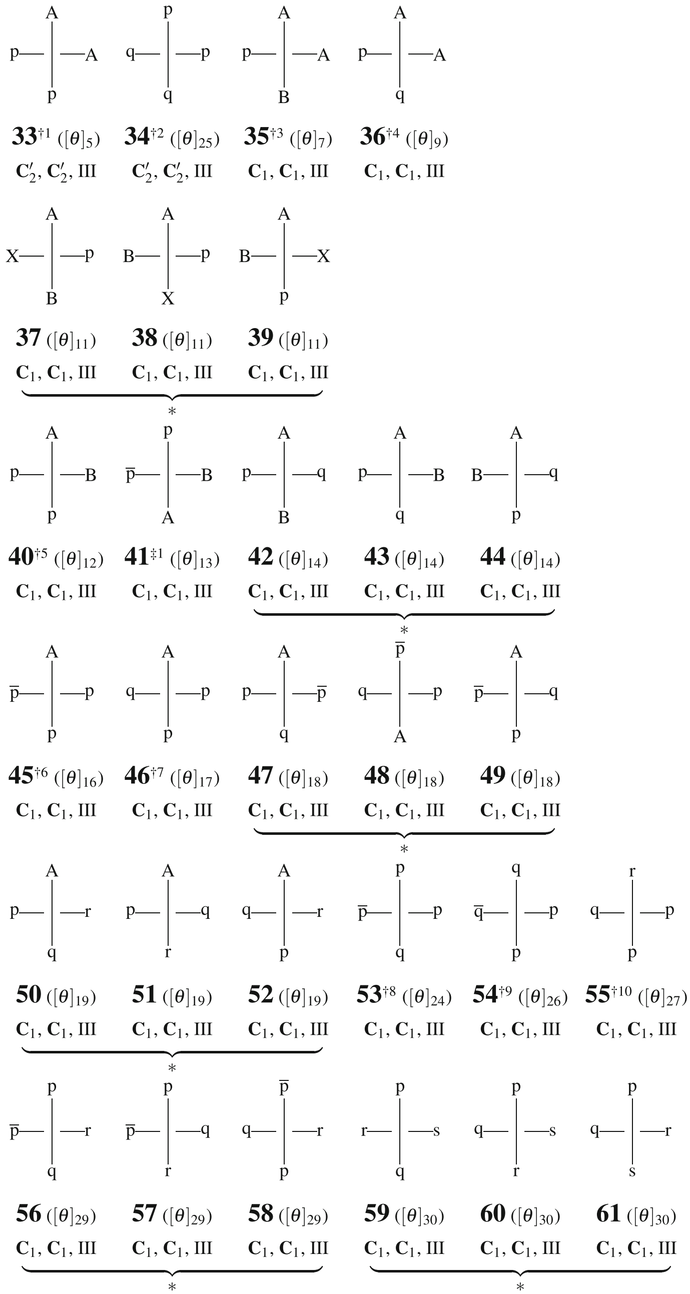

Fig. 8 Representatives of type-III quadruplets for allene derivatives. The partitions $[\theta]_i$ (i = 1–30) are shown in Eqs. 68–97. The *RS*-stereoisomeric groups of type III are selected from Eqs. 27–30 in accord with enumeration data listed in ICM_1 (Eq. 111) and ICM_2 (Eq. 113). The *RS*-stereoisomeric groups are accompanies with the corresponding point groups (the same as the *RS*-stereoisomeric groups) and stereoisogram types

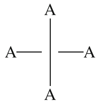

62 ($[\theta]_1$)
$\mathbf{D}_{2d\widetilde{\sigma}\widehat{I}}$, $\mathbf{D}_{2d}$, IV

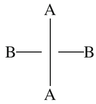

63[¶1] ($[\theta]_4$)
$\mathbf{C}_{2v\widetilde{\sigma}\widehat{I}}$, $\mathbf{C}_{2v}$, IV

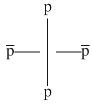

64[¶2] ($[\theta]_{23}$)
$\mathbf{S}_{4\widetilde{\sigma}\widehat{\sigma}}$, $\mathbf{S}_4$, IV

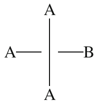

65 ($[\theta]_2$)
$\mathbf{C}_{s\widetilde{\sigma}\widehat{I}}$, $\mathbf{C}_s$, IV

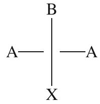

66[¶3] ($[\theta]_6$)
$\mathbf{C}_{s\widetilde{\sigma}\widehat{I}}$, $\mathbf{C}_s$, IV

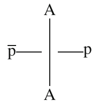

67[¶4] ($[\theta]_8$)
$\mathbf{C}_{s\widetilde{\sigma}\widehat{\sigma}}$, $\mathbf{C}_s$, IV

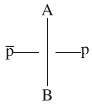

68[‡1] ($[\theta]_{13}$)
$\mathbf{C}_s$, $\mathbf{C}_s$, V

Fig. 9 Representatives of type-IV and type-V quadruplets for allene derivatives. The partitions $[\theta]_i$ ($i = 1$–30) are shown in Eqs. 68–97. The *RS*-stereoisomeric groups of type IV or type V are selected from Eqs. 47–53 or Eqs. 31–34 in accord with enumeration data listed in ICM_1 (Eq. 111) and ICM_2 (Eq. 113). The *RS*-stereoisomeric groups are accompanies with the corresponding point groups and stereoisogram types

first column) and $\mathbf{C}'_2$ (the third column). A reference promolecule for each enumerated quadruplet is depicted in Fig. 8.

For example, the promolecule **33** of type III ($\mathrm{A}^2\mathrm{p}^2$), which corresponds to the partition $[\theta]_5$, is an isoskeletal isomer of the promolecule **19** of type II, as denoted by the symbol †1. The promolecule **33** belongs to the *RS*-stereoisomeric group $\mathbf{C}'_2$.

The value 1/2 at the intersection between the $[\theta]_5$-row and the $\mathbf{C}'_2$-column (the third column) of Eq. 111 shows the presence of one quadruplet of $\frac{1}{2}(\mathrm{A}^2\mathrm{p}^2 + \mathrm{A}^2\overline{\mathrm{p}}^2)$. The corresponding stereoisogram of type III is shown in Fig. 5, where a pair of **A** and $\overline{\mathbf{A}}$ or another pair of **B** and $\overline{\mathbf{B}}$ corresponds to $\mathrm{A}^2\mathrm{p}^2$ and $\mathrm{A}^2\overline{\mathrm{p}}^2$. The subduction at the third row of Table 3 indicates the presence of two $\mathbf{C}'_2(/\mathbf{C}_1)$-orbits which accommodate A^2 and p^2 separately.

As another example to be examined, the promolecule **41** of $\mathrm{ABp}\overline{\mathrm{p}}$ ($[\theta]_{13}$) belongs to the *RS*-stereoisomeric group $\mathbf{C}_1$, which gives a type-III stereoisogram. The presence of one *RS*-stereoisomer is confirmed by the value 1 appearing at the intersection between the $[\theta]_{13}$-row and the $\mathbf{C}_1$-column (the first column) of Eq. 111. The promolecule **41**, as attached by the symbol ‡1, corresponds to **68** with ‡1 (type V in Fig. 9), where the enumerated value of the latter appears at the intersection between the $[\theta]_{13}$-row and the $\mathbf{C}_s$-column (the 6th column) of Eq. 111.

Three promolecules linked with an underbrace (*) have the same partition but belong to different *RS*-stereoisomeric groups, although they are categorized into the same type (type III). For example, a set of **37**, **38**, and **39** exhibits isoskeletal isomerism within the type-III category, where its value 3/2 appearing in the $[\theta]_{11}$-row of Eq. 111 should be interpreted as $3 \times \frac{1}{2}(\mathrm{ABXp} + \mathrm{ABX}\overline{\mathrm{p}})$. Similar situations emerge for sets of **42/43/44** ($[\theta]_{14}$), **47/48/49** ($[\theta]_{18}$), **50/51/52** ($[\theta]_{19}$), **56/57/58** ($[\theta]_{29}$), and **59/60/61** ($[\theta]_{30}$).

Quadruplets of Type IV Among the subgroups listed in Eq. 117 (cf. Eqs. 47–53) for characterizing quadruplets of type-IV stereoisograms, the itemized enumerations shown in Eqs. 111 and 113 indicate that there appear quadruplets belonging to $\mathbf{C}_{s\widetilde{\sigma}\widehat{I}}$,

$\mathbf{C}_{s\widetilde{\sigma}\widehat{\sigma}}$, $\mathbf{S}_{4\widetilde{\sigma}\widehat{\sigma}}$, $\mathbf{C}_{2v\widetilde{\sigma}\widehat{I}}$, and $\mathbf{D}_{2d\widetilde{\sigma}\widehat{I}}$. A reference promolecule for each enumerated quadruplet is depicted in Fig. 9.

The promolecule **63** with ¶1, which is an isoskeletal isomer of **8** with ¶1 (type I in Fig. 6), belongs to the *RS*-stereoisomeric group $\mathbf{C}_{2v\widetilde{\sigma}\widehat{I}}$. The presence of one *RS*-stereoisomer is confirmed by the value 1 appearing at the intersection between the $[\theta]_4$-row and the $\mathbf{C}_{2v\widetilde{\sigma}\widehat{I}}$-column (the 25th column) of Eq. 111. The promolecule **63** is a representative of a type-IV stereoisogram shown in Fig. 5, which contains **A** as a sole promolecule.

The promolecule **64** with ¶2 ($[\theta]_{23}$) is an isoskeletal isomer of **9** with ¶2 (Fig. 6). The promolecule **64** belongs to the *RS*-stereoisomeric group $\mathbf{S}_{4\widetilde{\sigma}\widehat{\sigma}}$, which gives a type-IV stereoisogram shown in Fig. 5.

It should be noted that the four positions of **64** construct a four-membered $\mathbf{S}_{4\widetilde{\sigma}\widehat{\sigma}}(/\mathbf{C}_{\widetilde{\sigma}})$-orbit (cf. the 23rd row of Table 3), which is determined to be enantiospheric. Note that $\mathbf{S}_{4\widetilde{\sigma}\widehat{\sigma}}$ is ex-achiral and $\mathbf{C}_{\widetilde{\sigma}}$ is ex-chiral in terms of the *RS*-stereoisomeric-group theory. Hence, the four proligands $\mathrm{p}^2\overline{\mathrm{p}}^2$ are equivalent to one another under the action of $\mathbf{S}_{4\widetilde{\sigma}\widehat{\sigma}}$ ($\subset \mathbf{D}_{2d\widetilde{\sigma}\widehat{\sigma}}$).

From the viewpoint of the point-group theory, on the other hand, the four positions of **64** construct a four-membered $\mathbf{S}_4(/\mathbf{C}_1)$-orbit, which is determined to be enantiospheric. Note that $\mathbf{S}_4$ is achiral and $\mathbf{C}_1$ is chiral in terms of the point-group theory. Hence, the four proligands $\mathrm{p}^2\overline{\mathrm{p}}^2$ are also concluded to be equivalent to one another under the action of $\mathbf{S}_4$ ($\subset \mathbf{D}_{2d}$). The conventional term 'enantiotopic' should be extended to characterize such a four- or more-membered enantiospheric orbit.

Quadruplets of Type V Among the subgroups listed in Eq. 118 (cf. Eqs. 31–34) for characterizing quadruplets of type-V stereoisograms, the itemized enumerations shown in Eqs. 111 and 113 indicate the presence of one quadruplet at the intersection between the $[\theta]_{13}$-row and the $\mathbf{C}_s$-column (the 6th column). This quadruplet is represented by a reference promolecule **68** with ‡1 ($[\theta]_{13}$), which is an isoskeletal isomer of **41** with ‡1 (cf. Fig. 8). The reference promolecule **68** derives a type-V stereoisogram shown in Fig. 5, which contains achiral promolecules **A** and **B**. Note that the two achiral promolecules **A** and **B** are *RS*-diastereomeric to each other. The features of the type-V stereoisogram will be more detailedly discussed in Part II of this series.

In terms of the conventional terminology based on 'pseudoasymmetric axis' and 'chirality axis' (Table 1 of [41]), stereodescriptors '*r*/*s*' are assigned to such 'pseudoasymmetric axes' as **68** (type V, achiral) and **47** (type III, chiral), while stereodescriptors '*R*/*S*' are assigned to such 'chiral axes' as **8** (type I, chiral) and **33** (type III, chiral). In particular, the chiral case **47** (characterized to be a 'pseudoasymmetric' axis) is inconsistent with the dichotomy between the term 'pseudoasymmetric axis' and the term 'chirality axis'. It follows that the conventional terms 'pseudoasymmetric axis' should be restricted to such achiral cases as **68** (type V, achiral) if the dichotomy is maintained. After the abandonment of the dichotomy, however, the assignment of stereodescriptors '*r*/*s*' to **68** (type V, achiral) and **47** (type III, chiral) should be rationalized by a new formulation free from the conventional term 'pseudoasymmetric axis'. Note that 'pseudoasymmetry' (concerning *RS-stereogenicity* in the present terminology) and 'chirality' (concerning *chirality* in the present terminology) denote distinct categories from the present viewpoint. Such a new formulation will be more detailedly discussed in Part II of this series.

6 Type-itemized enumeration

6.1 Type-enumeration matrices

The categories shown in Eqs. 114–118 enable us to enumerate quadruplets in an itemized fashion with respect to the five types of stereoisograms. For this purpose, the type-enumeration matrix (TEM) is introduced in a parallel way to a gross-enumeration matrix (GEM) for gross enumerations (cf. Table 2 of the present paper).

Let $\overline{m}_{ji}$ be the ji-element of the inverse mark table $M^{-1}_{\mathbf{D}_{2d\widetilde{\sigma}\widehat{I}}}$ (Eq. 109). The $\acute{\mathbf{G}}_j$-row is tentatively fixed and the row is summed up according to the categorization of type I–V as follows:

$$\widehat{N}_j^{(I)} = \sum_{\acute{\mathbf{G}}_i \in \mathrm{SG}^{[\mathrm{I}]}} \overline{m}_{ji} \tag{119}$$

$$\widehat{N}_j^{(II)} = \sum_{\acute{\mathbf{G}}_i \in \mathrm{SG}^{[\mathrm{II}]}} \overline{m}_{ji} \tag{120}$$

$$\widehat{N}_j^{(III)} = \sum_{\acute{\mathbf{G}}_i \in \mathrm{SG}^{[\mathrm{III}]}} \overline{m}_{ji} \tag{121}$$

$$\widehat{N}_j^{(IV)} = \sum_{\acute{\mathbf{G}}_i \in \mathrm{SG}^{[\mathrm{IV}]}} \overline{m}_{ji} \tag{122}$$

$$\widehat{N}_j^{(V)} = \sum_{\acute{\mathbf{G}}_i \in \mathrm{SG}^{[\mathrm{V}]}} \overline{m}_{ji} \tag{123}$$

$$\widehat{N}_j = \widehat{N}_j^{(I)} + \widehat{N}_j^{(II)} + \widehat{N}_j^{(III)} + \widehat{N}_j^{(IV)} + \widehat{N}_j^{(V)} \tag{124}$$

Let us consider a 27×6 type-enumeration matrix (TEM) where the j-th row (TEM_j) as a row vector is represented as follows:

$$\mathrm{TEM}_j = \left(\widehat{N}_j, \widehat{N}_j^{(I)}, \widehat{N}_j^{(II)}, \widehat{N}_j^{(III)}, \widehat{N}_j^{(IV)}, \widehat{N}_j^{(V)}\right) \tag{125}$$

for $\acute{\mathbf{G}}_j$ ($\in \mathrm{SSG}_{\mathbf{D}_{2d\widetilde{\sigma}\widehat{I}}}$) (cf. Eq. 54). Then $\acute{\mathbf{G}}_j$ runs to cover the SSG (Eq. 54) so as to give 27 row vectors TEM_j ($j = 1$–27). The respective elements of TEM_j are collected in the TEM column of Table 3.

Because the FPM_1 (Eq. 110) contains FPVs as its row vectors, it is multiplied by the TEM (Eq. 125 and Table 3) so as to give an isomer-type-counting matrix (ITCM), where the six columns contain the numbers of total quadruplets and those of quadruplets of the respective types.

$$\mathrm{ITCM}_1 = \mathrm{FPM}_1 \times \textsc{tem} = \begin{array}{c} [\theta]_1 \\ [\theta]_2 \\ [\theta]_3 \\ [\theta]_4 \\ [\theta]_5 \\ [\theta]_6 \\ [\theta]_7 \\ [\theta]_8 \\ [\theta]_9 \\ [\theta]_{10} \\ [\theta]_{11} \\ [\theta]_{12} \\ [\theta]_{13} \\ [\theta]_{14} \\ [\theta]_{15} \\ [\theta]_{16} \\ [\theta]_{17} \\ [\theta]_{18} \\ [\theta]_{19} \end{array} \left[\begin{array}{cccccc} 1 & 0 & 0 & 0 & 1 & 0 \\ 1 & 0 & 0 & 0 & 1 & 0 \\ 1/2 & 0 & 1/2 & 0 & 0 & 0 \\ 2 & 1 & 0 & 0 & 1 & 0 \\ 1 & 0 & 1/2 & 1/2 & 0 & 0 \\ 2 & 1 & 0 & 0 & 1 & 0 \\ 1 & 0 & 1/2 & 1/2 & 0 & 0 \\ 2 & 1 & 0 & 0 & 1 & 0 \\ 1 & 0 & 1/2 & 1/2 & 0 & 0 \\ 3 & 3 & 0 & 0 & 0 & 0 \\ 3/2 & 0 & 0 & 3/2 & 0 & 0 \\ 1 & 0 & 1/2 & 1/2 & 0 & 0 \\ 2 & 0 & 0 & 1 & 0 & 1 \\ 3/2 & 0 & 0 & 3/2 & 0 & 0 \\ 1/2 & 0 & 1/2 & 0 & 0 & 0 \\ 1 & 0 & 1/2 & 1/2 & 0 & 0 \\ 1 & 0 & 1/2 & 1/2 & 0 & 0 \\ 3/2 & 0 & 0 & 3/2 & 0 & 0 \\ 3/2 & 0 & 0 & 3/2 & 0 & 0 \end{array} \right] \tag{126}$$

In a similar way, the FPM_2 (Eq. 112) contains FPVs as its row vectors. The matrix is multiplied by the TEM (Eq. 125 and Table 3) so as to give an isomer-type-counting matrix (ITCM), where the six columns contain the numbers of total quadruplets and of quadruplets of respective types.

$$\mathrm{ITCM}_2 = \mathrm{FPM}_2 \times \textsc{tem} = \begin{array}{c} [\theta]_{20} \\ [\theta]_{21} \\ [\theta]_{22} \\ [\theta]_{23} \\ [\theta]_{24} \\ [\theta]_{25} \\ [\theta]_{26} \\ [\theta]_{27} \\ [\theta]_{28} \\ [\theta]_{29} \\ [\theta]_{30} \end{array} \left[\begin{array}{cccccc} 1/2 & 0 & 1/2 & 0 & 0 & 0 \\ 1/2 & 0 & 1/2 & 0 & 0 & 0 \\ 1/2 & 0 & 1/2 & 0 & 0 & 0 \\ 2 & 1 & 0 & 0 & 1 & 0 \\ 1 & 0 & 1/2 & 1/2 & 0 & 0 \\ 1 & 0 & 1/2 & 1/2 & 0 & 0 \\ 1 & 0 & 1/2 & 1/2 & 0 & 0 \\ 1 & 0 & 1/2 & 1/2 & 0 & 0 \\ 3 & 3 & 0 & 0 & 0 & 0 \\ 3/2 & 0 & 0 & 3/2 & 0 & 0 \\ 3/2 & 0 & 0 & 3/2 & 0 & 0 \end{array} \right] \tag{127}$$

The values collected in the ITCMs (Eqs. 126 and 127) are consistent with the quadruplets listed in Figs. 6–9, i.e., the second columns (type I) with Fig. 6, the third columns (type II) with Fig. 7, the 4th columns (type III) with Fig. 8, the 5th columns (type IV) with the top two rows of Fig. 6, and the 6th columns (type V) with the bottom row of Fig. 8. For example, the value 1/2 at the intersection of the $[\theta]_3$-row and the third column (the type-II column) in Eq. 126 corresponds to the term $\frac{1}{2}(\mathrm{A}^3\mathrm{p} + \mathrm{A}^3\overline{\mathrm{p}})$. This term indicates the presence of a quadruplet of *RS*-stereoisomers (as a pair of enantiomers) with the partition $[\theta]_3$, where the $\mathbf{C}_{\widetilde{\sigma}}$-promolecule **21** is a representative of the quadruplet characterized by the type-II stereoisogram shown in Fig. 7.

The values calculated in Eqs. 126 and 127 under the action of the *RS*-stereoisomeric group $\mathbf{D}_{2d\widetilde{\sigma}\widehat{I}}$ are consistent with the previous results enumerated under the action of the corresponding point group $\mathbf{D}_{2d}$ [38].

7 Conclusion

The isomorphism between the *RS*-stereoisomeric group $\mathbf{D}_{2d\widetilde{\sigma}\widehat{I}}$ and the point group $\mathbf{D}_{4h}$ has been throughly discussed, so as to clarify the subgroups of $\mathbf{D}_{2d\widetilde{\sigma}\widehat{I}}$. After the coset representation of $\mathbf{D}_{2d\widetilde{\sigma}\widehat{I}}$ is subduced to the subgroups, unit-subduced cycle indices with chirality fittingness (USCI-CFs) for characterizing $\mathbf{D}_{2d\widetilde{\sigma}\widehat{I}}$ are obtained according to the USCI approach developed by Fujita [11]. Then, the FPM method of the USCI approach is applied to the USCI-CFs. Thereby, the numbers of quadruplets are calculated in an itemized fashion with respect to the subgroups of $\mathbf{D}_{2d\widetilde{\sigma}\widehat{I}}$. After the subgroups of $\mathbf{D}_{2d\widetilde{\sigma}\widehat{I}}$ are categorized into types I to V, type-itemized enumeration of quadruplets is conducted to illustrate the versatility of the stereoisogram approach.

References

1. H.H. Jaffé, M. Orchin, *Symmetry in Chemistry* (Wiley, Chichester, 1965)
2. D.M. Bishop, *Group Theory and Chemistry* (Clarendon, Oxford, 1973)
3. E.L. Eliel, S.H. Wilen, *Stereochemistry of Organic Compounds* (Wiley, New York, 1994)
4. F.A. Cotton, *Chemical Applications of Group Theory* (Wiley-International, New York, 1990)
5. L.H. Hall, *Group Theory and Symmetry in Chemistry* (McGraw-Hill, New York, 1969)
6. S. Fujita, Theor. Chim. Acta **78**, 45–63 (1990)
7. S. Fujita, *Combinatorial Enumeration of Graphs, Three-Dimensional Structures, and Chemical Compounds* (University of Kragujevac, Faculty of Science, Kragujevac, 2013)
8. S. Fujita, Bull. Chem. Soc. Jpn. **63**, 315–327 (1990)
9. S. Fujita, J. Am. Chem. Soc. **112**, 3390–3397 (1990)
10. K. Mislow, M. Raban, Top. Stereochem. **1**, 1–38 (1967)
11. S. Fujita, *Symmetry and Combinatorial Enumeration in Chemistry* (Springer, Berlin, 1991)
12. S. Fujita, Tetrahedron **47**, 31–46 (1991)
13. S. Fujita, J. Chem. Inf. Comput. Sci. **40**, 135–146 (2000)
14. S. Fujita, Bull. Chem. Soc. Jpn. **73**, 329–339 (2000)
15. S. Fujita, S. El-Basil, J. Math. Chem. **36**, 211–229 (2004)
16. S. Fujita, MATCH Commun. Math. Comput. Chem. **54**, 251–300 (2005)
17. S. Fujita, MATCH Commun. Math. Comput. Chem. **55**, 5–38 (2006)
18. S. Fujita, MATCH Commun. Math. Comput. Chem. **55**, 237–270 (2006)
19. S. Fujita, *Diagrammatical Approach to Molecular Symmetry and Enumeration of Stereoisomers* (University of Kragujevac, Faculty of Science, Kragujevac, 2007)
20. S. Fujita, Theor. Chem. Acc. **113**, 73–79 (2005)
21. S. Fujita, MATCH Commun. Math. Comput. Chem. **57**, 5–48 (2007)
22. S. Fujita, J. Math. Chem. **42**, 481–534 (2007)
23. S. Fujita, Bull. Chem. Soc. Jpn. **75**, 1949–1962 (2002)
24. S. Fujita, J. Math. Chem. **33**, 113–143 (2003)
25. S. Fujita, J. Org. Chem. **69**, 3158–3165 (2004)
26. S. Fujita, J. Math. Chem. **35**, 265–287 (2004)
27. S. Fujita, Tetrahedron **60**, 11629–11638 (2004)
28. S. Fujita, MATCH Commun. Math. Comput. Chem. **61**, 11–38 (2009)
29. S. Fujita, J. Comput. Aided Chem. **10**, 16–29 (2009)
30. S. Fujita, Stereoisograms: a remedy against oversimplified dichotomy between enantiomers and diastereomers in stereochemistry, in *Chemical Information and Computational Challenge in the 21st Century*, ed. by M.V. Putz (Nova, New York 2012) Chapter 9, pp. 223–242.
31. S. Fujita, Tetrahedron **62**, 691–705 (2006)
32. S. Fujita, Yuki Gosei Kagaku Kyokai-Shi/J. Synth. Org. Chem. Jpn. **66**, 995–1004 (2008)
33. S. Fujita, MATCH Commun. Math. Comput. Chem. **61**, 39–70 (2009)
34. S. Fujita, J. Comput. Aided Chem. **10**, 76–95 (2009)
35. S. Fujita, Prochirality and pro-RS-stereogenicity. Stereoisogram Approach Free from the Conventional "Prochirality" and "Prostereogenicity", in *Carbon Bonding and Structures. Advances in Physics and Chemistry*, ed. by M. V. Putz (Springer, Dordrecht, Heidelberg, London 2011) Vol. 5 of Carbon Materials: Chemistry and Physics Chapter 10, pp. 227–271.
36. S. Fujita, MATCH Commun. Math. Comput. Chem. **52**, 3–18 (2004)
37. S. Fujita, MATCH Commun. Math. Comput. Chem. **54**, 39–52 (2005)

38. S. Fujita, Memoirs of the Faculty of Engineering and Design. Kyoto Inst. Technol. **53**, 19–38 (2005)
39. S. Fujita, Helv. Chim. Acta **85**, 2440–2457 (2002)
40. S. Fujita, MATCH Commun. Math. Comput. Chem. **61**, 71–115 (2009)
41. G. Helmchen, in *Stereoselective Synthesis*, 4 edn., ed. by G. Helmchen, R. W. Hoffmann, J. Mulzer, E. Schaumann, (Georg Thieme, Stuttgart New York 1996) Vol. 1 of Methods of Organic Chemistry (Houben-Weyl). Workbench Edition E21 pp 1–74